



Universiteit
Leiden
The Netherlands

Unfolding symmetric Bogdanov-Takens bifurcations for front dynamics in a reaction-diffusion system

Chirilus-Bruckner, M.; Heijster, P. van; Ikeda, H.; Rademacher, J.D.M.

Citation

Chirilus-Bruckner, M., Heijster, P. van, Ikeda, H., & Rademacher, J. D. M. (2019). Unfolding symmetric Bogdanov-Takens bifurcations for front dynamics in a reaction-diffusion system. *Journal Of Nonlinear Science*, 29, 2911-2953. doi:10.1007/s00332-019-09563-2

Version: Publisher's Version

License: [Licensed under Article 25fa Copyright Act/Law \(Amendment Taverne\)](#)

Downloaded from: <https://hdl.handle.net/1887/3248625>

Note: To cite this publication please use the final published version (if applicable).



Unfolding Symmetric Bogdanov–Takens Bifurcations for Front Dynamics in a Reaction–Diffusion System

M. Chirilus-Bruckner¹ · P. van Heijster² · H. Ikeda³ · J. D. M. Rademacher⁴ 

Received: 25 January 2019 / Accepted: 2 July 2019 / Published online: 16 August 2019
© Springer Science+Business Media, LLC, part of Springer Nature 2019

Abstract

This paper extends the analysis of a much studied singularly perturbed three-component reaction–diffusion system for front dynamics in the regime where the essential spectrum is close to the origin. We confirm a conjecture from a preceding paper by proving that the triple multiplicity of the zero eigenvalue gives a Jordan chain of length three. Moreover, we simplify the center manifold reduction and computation of the normal form coefficients by using the Evans function for the eigenvalues. Finally, we prove the unfolding of a Bogdanov–Takens bifurcation with symmetry in the model. This leads to the appearance of stable periodic front motion, including stable traveling breathers, and these results are illustrated by numerical computations.

Keywords Three-component reaction–diffusion system · Front solution · Singular perturbation theory · Evans function · Center manifold reduction · Normal forms

Mathematics Subject Classification 35C07 · 37L10 · 35K57 · 34D15

Communicated by Dr. Alain Goriely.

PvH was supported under the Australian Research Council’s Discovery Early Career Researcher Award funding scheme DE140100741. HI was partially supported by JSPS KAKENHI Grant Number JP15K04885 and JST CREST Grant Number JPMJCR14D3. JR was supported in part by DFG Grant Ra 2788/1-1 and TRR 181 Project Number 274762653.

✉ J. D. M. Rademacher
jdmr@uni-bremen.de

¹ Mathematisch Instituut, Leiden University, P.O. Box 9512, 2300 RA Leiden, The Netherlands

² Mathematical Sciences School, Queensland University of Technology, GPO Box 2434, Brisbane, QLD 4001, Australia

³ Department of Mathematics, University of Toyama, Gofuku 3190, Toyama 930-8555, Japan

⁴ Fachbereich Mathematik, Universität Bremen, Postfach 22 04 40, 20359 Bremen, Germany

1 Introduction

Localized structures, such as fronts, pulses, stripes and spots, are close to spatially homogeneous states except for relatively small regions in space. Here, a transition between different homogeneous states, or a local excursion, occurs. Such localized structures often form the backbone of more complex patterns in reaction–diffusion equations (e.g., Hagberg and Meron 1994; Nishiura and Ueyama 2001; Pearson 1993) so that understanding localized structures is a crucial step toward understanding complex patterns. While significant progress has been made over the past few decades to understand localized structures, see, e.g., Bellsky et al. (2014), Doelman and Kaper (2003), Doelman et al. (2007), Ei et al. (2002), Kolokolnikov et al. (2006), Promislow (2002), Rademacher (2013), Sandstede (2002), Sun et al. (2005), and references therein, many open questions remain.

One of these concerns the influence of the essential spectrum on bifurcations as it approaches the imaginary axis. This question is the main motivation of the current paper, which continues the investigation of Chirilus-Bruckner et al. (2015) on front bifurcations for nearly critical essential spectrum. Here, the localized structures are fronts, which are singular perturbations of sharp interfaces of the Allen–Cahn equation coupled to linear large-scale fields, and we view this as a caricature model for multiscale effects on interfacial dynamics and energy transfer. There is a large body of literature on related models and also planar fronts with a more physical perspective, e.g., Meron et al. (2001), Meron (2015), and the references therein.

We take a mathematical viewpoint and consider the three-component singularly perturbed reaction–diffusion system

$$\begin{cases} \partial_t U = \varepsilon^2 \partial_x^2 U + U - U^3 - \varepsilon(\alpha V + \beta W + \gamma), \\ \frac{\hat{\tau}}{\varepsilon^2} \partial_t V = \partial_x^2 V + U - V, \\ \frac{\hat{\theta}}{\varepsilon^2} \partial_t W = D^2 \partial_x^2 W + U - W, \end{cases} \quad (1)$$

with $x \in \mathbb{R}$, $t \geq 0$, $U = U(x, t)$, $V = V(x, t)$, $W = W(x, t) \in \mathbb{R}$, and parameters $\alpha, \beta, \gamma \in \mathbb{R}$, $\hat{\tau}, \hat{\theta} > 0$, $D > 1$,¹ as well as the singular perturbation scale $0 < \varepsilon \ll 1$ such that all parameters, including $\hat{\tau}, \hat{\theta}$, are $\mathcal{O}(1)$ with respect to ε . A dimensional version of this system was introduced in the mid-nineties to study gas-discharge systems on a phenomenological level (e.g., Or-Guil et al. 1998; Purwins and Stollenwerk 2014; Schenk et al. 1997). Afterward, versions of (1) have been studied extensively by mathematicians since it supports localized solutions that undergo complex dynamics while the model is still amendable for rigorous analysis (e.g., Chen and Choi 2012; Chirilus-Bruckner et al. 2015; Doelman et al. 2009; Nishiura et al. 2003, 2007; van Heijster et al. 2018, 2019, 2008, 2010, 2011; van Heijster and Sandstede 2011, 2014; Vanag and Epstein 2007). In the predecessor paper (Chirilus-Bruckner et al. 2015), it was shown that system (1) supports uniformly traveling front solutions

¹ The condition $D > 1$ implies that the W -component has the largest diffusion coefficient and its profile thus changes the slowest (as function of the spatial variable x), see for instance Fig. 1. This condition stems from the original gas-discharge system and is not a mathematically necessary requirement, though convenient. For $D < 1$ the W -component and the V -component simply interchange roles.

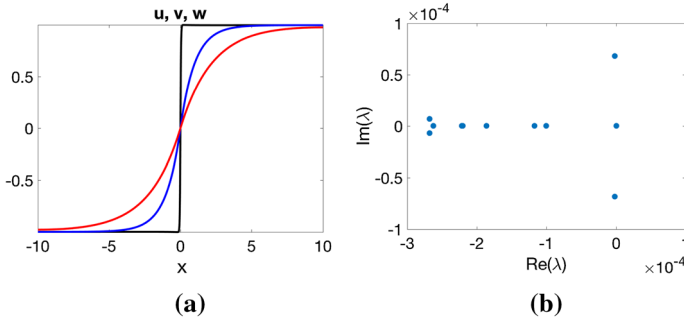


Fig. 1 **a** Sample profile of a numerically computed stationary front solution near a Hopf bifurcation with the profiles of u (black) v (blue) and w (red); parameter values are those of Fig. 4 with $g_2 \approx -0.003$. **b** Spectrum of this front with gap between the leading three eigenvalues as theoretically predicted

$(U, V, W)(x, t) = (u^{tf}, v^{tf}, w^{tf})(x - \varepsilon^2 ct)$ that transition from the background state near $(-1, -1, -1)$ to the background state near $(1, 1, 1)$ if the system parameters and the velocity c satisfy the existence condition

$$\Gamma_\varepsilon(c) = \alpha \frac{c\hat{t}}{\sqrt{c^2\hat{t}^2 + 4}} + \beta \frac{c\hat{\theta}}{D\sqrt{c^2\frac{\hat{\theta}^2}{D^2} + 4}} + \gamma - \frac{\sqrt{2}}{3}c + h.o.t. = 0; \quad (2)$$

here and below ‘h.o.t’ abbreviates ‘higher-order terms,’ see Chirilus-Bruckner et al. (2015).

This condition trivially yields γ as a function of the remaining parameters and c , but for the partial differential equation (PDE) dynamics it is decisive to view Γ as a function of the auxiliary velocity parameter c . For $\gamma = 0$, the existence condition is an odd function of c , and for $\gamma \neq 0$, parameters can always be adjusted to find a traveling front solution with $c \neq 0$. Having in mind the symmetry breaking nature of γ in (1), we will focus on $\gamma = 0$ for the analysis of this paper. From the viewpoint of the Allen–Cahn energy, $\gamma \neq 0$ is a nontrivial external energy flux so that traveling fronts with nonzero velocity for $\gamma = 0$ are somewhat surprising, cf., e.g., Ikeda et al. (1989) and Nishiura et al. (1990). Typically, the energy flux $\gamma \neq 0$ is transferred to interface motions, which, as we shall prove, can also be oscillatory due to the coupled fields. It is well known that the stationary front solutions can undergo stationary bifurcations, and the full analysis of the bifurcation structure in Chirilus-Bruckner et al. (2015) yields a (partially unfolded) butterfly catastrophe.

Using geometric singular perturbation theory, the stationary front solutions to (1) can be specified to leading order in the perturbation parameter ε as

$$\begin{bmatrix} U(x, t) \\ V(x, t) \\ W(x, t) \end{bmatrix} = \begin{bmatrix} u^h(x) \\ v^h(x) \\ w^h(x) \end{bmatrix} = \begin{bmatrix} u_0^h(x) \\ v_0^h(x) \\ w_0^h(x) \end{bmatrix} + h.o.t., \quad (3)$$

with

$$\begin{bmatrix} u_0^h(x) \\ v_0^h(x) \\ w_0^h(x) \end{bmatrix} = \begin{bmatrix} \tanh\left[\frac{x}{\sqrt{2\varepsilon}}\right] \\ 0 \\ 0 \end{bmatrix} \chi_f(x) + \sum_{\sigma \in \{+, -\}} \sigma \begin{bmatrix} 1 \\ 1 - e^{-\sigma x} \\ 1 - e^{-\sigma x/D} \end{bmatrix} \chi_{s\sigma}(x)$$

and where the slow/large-scale and fast/small-scale behavior has been captured through

$$\chi_{s-} = \chi(-\infty, -\sqrt{\varepsilon}), \quad \chi_f = \chi[-\sqrt{\varepsilon}, +\sqrt{\varepsilon}], \quad \chi_{s+} = \chi(+\sqrt{\varepsilon}, +\infty).$$

It has been shown in Chirilus-Bruckner et al. (2015) that the operator arising from the linearization of (1) around a stationary front has the following spectral properties, also illustrated in Fig. 1b: First, its essential spectrum is located in a sector of the left half plane and bounded away from the imaginary axis by $\max\{-2, -\varepsilon^2/\hat{\tau}, -\varepsilon^2/\hat{\theta}\}$. Second, the only point spectrum that could lead to instabilities is small eigenvalues $\lambda = \varepsilon^2 \hat{\lambda}$. As usual for translation symmetric PDE, one such eigenvalue is $\lambda = 0$ with eigenfunction being the spatial derivative of the stationary front. Third, the algebraic multiplicity of $\lambda = 0$ can only be one, two or three, see also the upcoming Proposition 1.²

In Chirilus-Bruckner et al. (2015), the nonlinear stability analysis and bifurcations of stationary fronts have been treated for the special case of unfolding around a double zero eigenvalue. The more challenging case of unfolding the triple zero was left as an open problem, and is the topic of the present paper. We will use center manifold analysis in the vicinity of a triple zero eigenvalue to derive the dynamics of pseudo-front solutions with non-uniform speed $c = c(t)$.

We informally summarize the main results of this paper.

- *Linear structure* We provide an expansion for the existence problem of generalized eigenfunctions in the singular perturbation parameter and infer that, at criticality, the generalized kernel has a maximal Jordan chain.
- *Reduced vector field* We provide an explicit expansion of the reduced vector field on the center manifold. This entails the identification of the maximal degeneracies as a symmetric Bogdanov–Takens point with either a butterfly imprint, or a mixed cubic term degeneracy.
- *Unfolding* We prove the parameters unfold the symmetric Bogdanov–Takens case without further degeneracy, and analyze this case in detail. Direct numerical simulations of the PDE and numerical continuation corroborate and illustrate these results.
- *Symmetry breaking* The unfolding proves the existence of stable standing ‘breather’ solutions based on single fronts, cf. Fig. 2c. By symmetry breaking, we additionally infer the existence of stable ‘traveling breathers’ with nonzero average speed, also based on single fronts. See Fig. 2f. Being a mix of drift and

² Two of these eigenvalues have emerged from the essential spectrum upon increasing $\hat{\tau}$ and/or $\hat{\theta}$ from $\mathcal{O}(\varepsilon^2)$ to $\mathcal{O}(1)$, see van Heijster et al. (2008).

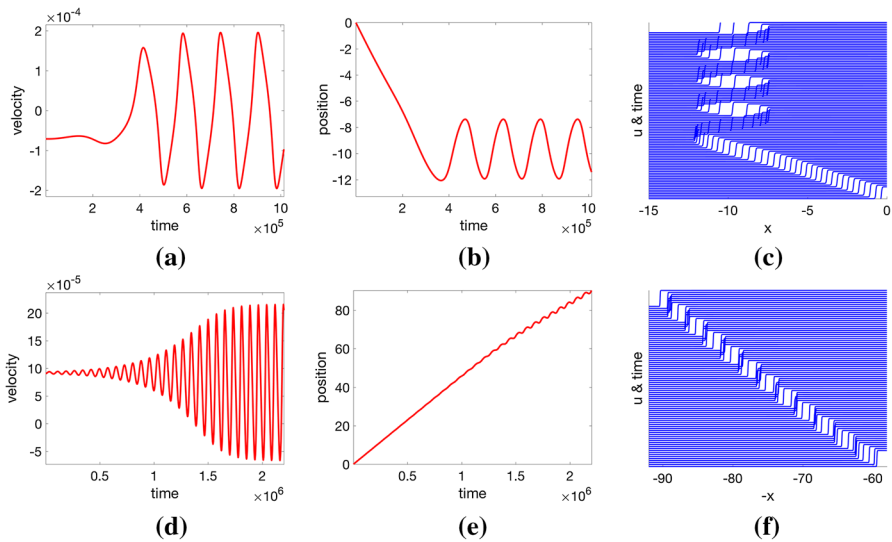


Fig. 2 Plots of velocities (**a**, **d**) and two views of positions of pseudo-fronts obtained from numerical simulations of (1) for parameters located by using the center manifold analysis. The solutions correspond to heteroclinic orbits from an equilibrium to a periodic orbit in the center manifold, see Sect. 3.3 for details. **a–c**: a perturbation of an unstable stationary front leads to a periodic front motion in both velocity and position, see Fig. 5. **d–f**: non-periodic positions, i.e., a ‘traveling breather,’ occurs due to $\gamma \neq 0$, see Fig. 7. **f** shows a subset from **e** and reflected for better view

oscillation, the latter are particularly interesting, also from the viewpoint of energy transfer.

We emphasize that the solutions of the ordinary differential equation (ODE) on the center manifold, as sketched in the upcoming Fig. 3, possess specific spatio-temporal forms for the PDE dynamics, cf. Fig. 2. These are organized around the standing front, which is the basic equilibrium state of this ODE. The Bogdanov–Takens unfolding entails Hopf bifurcations to periodic solutions, which – in the ODE phase plane – encircle the stationary front solution and thus create breather-like dynamics in the PDE by essentially moving the front back and forth periodically, cf. Fig. 3(2). This is more pronounced in the continuation of these periodic orbits beyond a pitchfork bifurcation of the standing front, where these encircle the standing front and a pair of equilibria that correspond to traveling fronts in opposite directions, cf. Fig. 3(3) and the PDE simulations in Fig. 2a–c. As a signature of the Bogdanov–Takens point, also homoclinic solutions and some heteroclinic connections emerge that can be interpreted similarly.

The term breather usually refers to periodically moving pulses rather than our case of a single front. They predominantly come as sharp spikes or broader plateaus built from opposing fronts. A rigorous treatment for the former can be found in the recent paper by Veerman (2015). The latter case relates to our situation, and early numerical as well as analytical studies on bounded domains can be found in Hagberg and Meron (1994) and Nishiura and Mimura (1989), where also the crossing of complex conjugate eigenvalues through the imaginary axis has been shown. Analogous results for

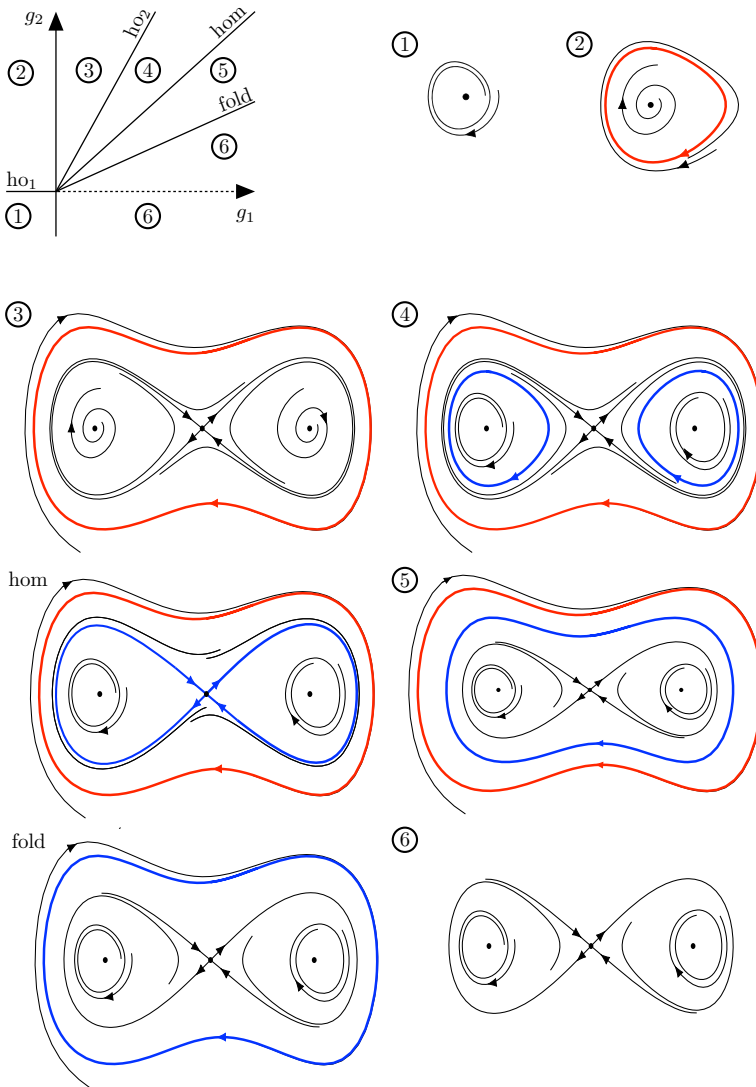


Fig. 3 Bifurcation diagram, and sketches of the associated phase planes, of a symmetric Bogdanov–Takens point in the case $g_3, g_4 < 0$. The periodic orbits plotted in red are stable, those in blue unstable. See also Figures 2 and 4 from Carr (1981)

unbounded domains were obtained in Ikeda and Ikeda (2000) and Ikeda et al. (2000). Breathers made of opposing fronts in our model were numerically found in Doelman et al. (2009), and a single breathing front was found in Chirilus-Bruckner et al. (2015). In the latter also the crossing of eigenvalues through the imaginary axis was proven. However, we are not aware of a rigorous treatment of the nonlinear unfolding of a Hopf bifurcation or the existence of standing or moving breathers of front-type in any of these cases.

In this paper, the aforementioned results for the symmetric Bogdanov–Takens case are based on showing that the front positions $a(t)$ satisfy an ODE of the form

$$\frac{d^3}{dt^3}a = \varepsilon^6 G(\dot{a}, \ddot{a}, \mu),$$

where μ combines system parameters used for unfolding the bifurcations—we eventually use $\mu = (\alpha, \beta)$ for convenience. The invariant subsystem for the velocities c , with $\varepsilon^2 c = \dot{a}$, on the slow time scale $' = \varepsilon^{-2} d/dt$ has the normal form

$$c'' = g_1(\mu)c + g_{30}c^3 + c' \left(g_2(\mu) + g_{40}c^2 \right)$$

and we provide explicit formulas for g_{30} , g_{40} , so as to ensure the non-degeneracy $g_{30}g_{40} \neq 0$ and the relevant expansion of g_1 , g_2 with respect to μ .

We close the introduction with some comments on the methods and techniques used in this paper. While the use of center manifold reduction is by now standard for instabilities caused by point spectrum, the main novelties of the article are as follows.

First, although the algebraic multiplicity three of the zero eigenvalue can easily be read off from the Evans function, see Proposition 1, the corresponding eigenspace needs more analysis. Formal computations, as demonstrated in Appendix A, suggest a Jordan block of length three arises and, hence, that there are two generalized eigenfunctions. We confirm this by an abstract rigorous argument for the existence of generalized eigenfunctions, which deals also with the asymptotic criticality of the essential spectrum as $\varepsilon \rightarrow 0$. Generally, there are two different methods for solving the singularly perturbed linearized eigenvalue problem: an analytical approach, the Singular Limit Eigenvalue Problem (SLEP) method (cf., Nishiura and Fujii 1987; Nishiura et al. 1990), and a geometrical approach, the Nonlocal Eigenvalue Problem (NLEP) method (cf. Doelman et al. 2001). Although both methods are based on the linearized stability principle, the former solves the linearized eigenvalue problem directly and derives a well-defined singular limit equation, the SLEP-equation, as $\varepsilon \rightarrow 0$. The latter method defines the Evans function (cf. Alexander et al. 1990) for the linearized equations and proceeds with a geometric or topological analysis. The SLEP-method gives very detailed information on the behavior of the critical eigenvalues for small ε , whereas the NLEP-method can be applied to wider class of equations. Here, we use the SLEP-method to find generalized eigenfunctions corresponding to the triple zero eigenvalue. This is slightly different from a usual eigenvalue problem because the zero eigenvalue has been determined previously, but it is the same in spirit: We find the relation between the system parameters included in the original eigenvalue problem and an eigenfunction, and this relation corresponds to an eigenvalue. This is also the crux to finding generalized eigenfunctions, and these relations play, in essence, the role of solvability conditions. In fact, we expect our results can be further generalized to extensions of (1) that lead to Jordan chains of arbitrary length, see Sect. 4.

Second, and more relevant for analyzing the concrete PDE dynamics, we circumvent the straightforward, but tedious computation of normal form coefficients of the usual center manifold reduction procedure by using the information on existence and stability of uniformly traveling fronts. We believe this strategy is of interest beyond our setting.

This paper is organized as follows. In Sect. 2, we discuss the results from Chirilus-Bruckner et al. (2015) and show that the operator arising from linearization around a stationary front of (1) possesses a Jordan chain of length three and we compute, to leading order, the second generalized eigenfunction. In Sect. 3, we use center manifold analysis in the vicinity of a triple zero eigenvalue to derive, and subsequently study, the dynamics of pseudo-front solutions with non-uniform speed $c = c(t)$. We end with a discussion of potential directions for future work.

2 Stability and Eigenfunctions of Stationary Front Solutions

In order to state results on the stability of stationary fronts, it is convenient to write our system (1) in the more concise form

$$M(\hat{\tau}, \hat{\theta})\partial_t Z = F(Z; \alpha, \beta, D),$$

where M, F are, with explicit ε -dependence, given by

$$M(\hat{\tau}, \hat{\theta}; \varepsilon) = \begin{pmatrix} 1 & 0 & 0 \\ 0 & \frac{\hat{\tau}}{\varepsilon^2} & 0 \\ 0 & 0 & \frac{\hat{\theta}}{\varepsilon^2} \end{pmatrix}, \quad \text{and} \quad (4)$$

$$F(Z; \alpha, \beta, D; \varepsilon) = \begin{pmatrix} \varepsilon^2 \partial_x^2 Z^u + Z^u - (Z^u)^3 - \varepsilon(\alpha Z^v + \beta Z^w) \\ \partial_x^2 Z^v - Z^v + Z^u \\ D^2 \partial_x^2 Z^w - Z^w + Z^u \end{pmatrix}.$$

Linearization around the stationary front $Z^{\text{sf}} = (u^h, v^h, w^h)$ from (3) gives rise to the eigenvalue problem

$$\lambda M(\hat{\tau}, \hat{\theta})\Phi = \partial_Z F(Z^{\text{sf}}; \alpha, \beta, D)\Phi,$$

so, in the following, we will be interested in the spectrum of the operator

$$\mathcal{L} := M(\hat{\tau}, \hat{\theta})^{-1} \partial_Z F(Z^{\text{sf}}; \alpha, \beta, D). \quad (5)$$

Various results on the critical eigenvalues and the corresponding eigenfunctions were obtained in Lemmas 5–8 and Corollary 3 from Chirilus-Bruckner et al. (2015), which we reformulate next. As we will see, unfolding the bifurcations can be realized with α, β, D , which is based on certain normal form coefficients introduced later. It is, however, instructive to first consider the quantities

$$\kappa_1^0 := \alpha \hat{\tau} + \beta \frac{\hat{\theta}}{D} - \frac{2\sqrt{2}}{3}, \quad \kappa_2^0 := \alpha \hat{\tau}^2 + \frac{\beta}{D} \hat{\theta}^2, \quad \kappa_3^0 := \alpha \hat{\tau}^3 + \beta \frac{\hat{\theta}^3}{D^3}, \quad (6)$$

which already appeared (Chirilus-Bruckner et al. 2015) and where the upper index 0 refers to $\varepsilon = 0$, the limit that forms the backbone of all our computations. Statements in terms of κ_j^0 , $j = 1, 2, 3$ thus implicitly refer to the parameters $\alpha, \beta, D, \hat{\tau}, \hat{\theta}$.

Proposition 1 (Stability of stationary front solutions, Chirilus-Bruckner et al. 2015) *Let $\varepsilon > 0$ be chosen sufficiently small. The critical spectrum of \mathcal{L} from (5) on $L^2(\mathbb{R})$ with domain $H^2(\mathbb{R})$, or $C_{\text{unif}}^0(\mathbb{R})$ with domain $C_{\text{unif}}^2(\mathbb{R})$, consists of at most three small eigenvalues $\lambda = \varepsilon^2 \hat{\lambda} + o(\varepsilon^2)$ given by the roots of the Evans function*

$$\mathcal{D}(\hat{\lambda}) := -\frac{\sqrt{2}}{3} \hat{\lambda} + \alpha \left(1 - \frac{1}{\sqrt{\hat{\tau} \hat{\lambda} + 1}} \right) + \frac{\beta}{D} \left(1 - \frac{1}{\sqrt{\hat{\theta} \hat{\lambda} + 1}} \right) = 0.$$

Furthermore, there are $\kappa_j^\varepsilon = \kappa_j^0 + O(\varepsilon)$, $j = 1, 2$, as in (6) and depending on the parameters $\alpha, \beta, D, \hat{\tau}, \hat{\theta}$, such that the following holds. For $0 < \varepsilon \ll 1$, the zero eigenvalue has multiplicity two if and only if

$$\begin{cases} \kappa_1^\varepsilon(\alpha, \beta, D, \hat{\tau}, \hat{\theta}) = 0, \\ \kappa_2^\varepsilon(\alpha, \beta, D, \hat{\tau}, \hat{\theta}) \neq 0, \end{cases} \tag{7}$$

while it has multiplicity three if and only if

$$\begin{cases} \kappa_1^\varepsilon(\alpha, \beta, D, \hat{\tau}, \hat{\theta}) = 0, \\ \kappa_2^\varepsilon(\alpha, \beta, D, \hat{\tau}, \hat{\theta}) = 0. \end{cases} \tag{8}$$

Hence, only small eigenvalues $\lambda = \varepsilon^2 \hat{\lambda}$ can lead to instabilities, so the relevant eigenvalue problem is scaled as

$$\varepsilon^2 \hat{\lambda} \tilde{\Phi} = \mathcal{L} \tilde{\Phi}, \tag{9}$$

with \mathcal{L} given by (5). As alluded to, without directly solving the eigenvalue problem, it is a priori clear that $\lambda = 0$ is an eigenvalue with eigenfunction given by $\partial_x Z^{\text{sf}}$. Furthermore, by varying parameters one can increase the algebraic multiplicity for the zero eigenvalue to two. In this case, we will have a corresponding Jordan block of length two since the generalized eigenfunction Ψ can be readily found from the smooth family of traveling front solutions Z^{tf} parameterized by the speed c : The existence problem $-\varepsilon^2 c Z^{\text{tf}} = M^{-1} F(Z^{\text{tf}})$ (where differentiation is meant with respect to the traveling wave coordinate $(x - \varepsilon^2 c)$) implies upon differentiation and evaluation at $c = 0$ that we have

$$-\varepsilon^2 \Phi = M^{-1} \partial_Z F(Z^{\text{sf}}) \partial_c Z^{\text{tf}}|_{c=0} + b = \mathcal{L} \Psi,$$

since $b = \frac{d}{dc} M^{-1} F(Z^{\text{sf}})|_{c=0} = 0$ at the double root, which coincides with the bifurcation point of steady states. The smoothness in ε at $\varepsilon = 0$ follows from the smoothness of $\varepsilon^2 \Phi$, so that the leading order form of the first generalized eigenfunction can also be found by performing a formal asymptotic expansion and matching, see Appendix A and, in particular, Lemma 6.

By further adjustment of the parameters, the algebraic multiplicity of the zero eigenvalue can be increased to three. Formal expansions (again as performed in Appendix A)

suggest the existence of a second generalized eigenfunction, since the corresponding solvability condition coincides with the triple zero eigenvalue condition. We give a rigorous proof of the occurrence of a Jordan block of length three similar to the SLEP-method, i.e., the ‘Singular Limit Eigenvalue Problem’ as developed and used in Nishiura and Fujii (1987) and Nishiura et al. (1990). It is quite possible that the existence of the second generalized eigenfunction can also be derived from the Evans function construction used to determine the algebraic multiplicity, though we do not pursue this here.

Proposition 2 (Jordan block structure for the zero eigenvalue) *Let $\varepsilon > 0$ be chosen sufficiently small and $\alpha, \beta, D, \hat{\tau}, \hat{\theta}$ fulfill (8) such that the zero eigenvalue of the operator*

$$\mathcal{L} := M(\hat{\tau}, \hat{\theta})^{-1} \partial_Z F(Z^{\text{sf}}; \alpha, \beta, D)$$

is algebraically triple. Then, \mathcal{L} possesses a Jordan chain of length 3. Specifically, let \mathcal{L}^ be the L^2 -adjoint operator of \mathcal{L} with respect to the duality product*

$$\langle Z, \tilde{Z} \rangle = \langle Z^u, \tilde{Z}^u \rangle_{L^2} + \langle Z^v, \tilde{Z}^v \rangle_{L^2} + \langle Z^w, \tilde{Z}^w \rangle_{L^2}.$$

Then, there are even functions $\Phi, \Psi, \tilde{\Psi}, \Phi^, \Psi^*, \tilde{\Psi}^*$ with*

$$\begin{aligned} \mathcal{L}\Phi &= 0, & \mathcal{L}\Psi &= \varepsilon^2\Phi, & \mathcal{L}\tilde{\Psi} &= \varepsilon^2\Psi, \\ \mathcal{L}^*\Phi^* &= 0, & \mathcal{L}^*\Psi^* &= \varepsilon^2\Phi^*, & \mathcal{L}^*\tilde{\Psi}^* &= \varepsilon^2\Psi^*. \end{aligned}$$

In particular,

$$\langle \Phi, \Phi^* \rangle = \langle \Phi, \Psi^* \rangle = \langle \Phi^*, \Psi \rangle = 0,$$

and for any fixed $p_1, p_2, p_3 \neq 0$ the (generalized) eigenfunctions $\Phi, \Psi, \tilde{\Psi}, \Phi^, \Psi^*, \tilde{\Psi}^*$ are uniquely determined by*

$$p_1 := \langle \Phi, \tilde{\Psi}^* \rangle, \quad p_2 := \langle \Psi, \tilde{\Psi}^* \rangle, \quad p_3 := \langle \tilde{\Psi}, \tilde{\Psi}^* \rangle. \tag{10}$$

Moreover, the parameters and (generalized) eigenfunctions lie in a continuous family with respect to $0 \leq \varepsilon \ll 1$.

Note that the Jordan chain relations imply $p_1 = \langle \Psi, \Psi^* \rangle = \langle \tilde{\Psi}, \Phi^* \rangle$ and $p_2 = \langle \tilde{\Psi}, \Psi^* \rangle$.

The following subsection forms the proof in several steps, which in fact reproves Proposition 1 with the SLEP-approach except for a non-degeneracy condition.

2.1 Existence of a Second Generalized Eigenfunction (Proof of Proposition 2)

Recall that the existence of an eigenfunction and a first generalized eigenfunction is already settled for $\kappa_1^\varepsilon = 0$, so there exist Φ, Ψ with $\mathcal{L}\Phi = 0, \mathcal{L}\Psi = \varepsilon^2\Phi$ (with

leading order expressions given in Appendix A; see also Remark 1). Hence, all we need to demonstrate is the existence of a second generalized eigenfunction $\tilde{\Psi}$ with

$$\mathcal{L}\tilde{\Psi} = \varepsilon^2\Psi. \tag{11}$$

Remark that $p_1, p_2, p_3 \neq 0$ in (10) are the normalization constants of the generalized eigenfunctions, which we keep unspecified for now.

Upon introducing the notation

$$\tilde{\Psi}_{v,w} = \begin{pmatrix} \tilde{\Psi}_v \\ \tilde{\Psi}_w \end{pmatrix}, \quad \Psi_{v,w} = \begin{pmatrix} \hat{\tau}\Psi_v \\ \hat{\theta}\Psi_w \end{pmatrix},$$

Equation (11) can be cast in terms of a block matrix operator as

$$\begin{pmatrix} L_\varepsilon & \varepsilon A \\ B & S \end{pmatrix} \begin{pmatrix} \tilde{\Psi}_u \\ \tilde{\Psi}_{v,w} \end{pmatrix} = \begin{pmatrix} \varepsilon^2\Psi_u \\ \Psi_{v,w} \end{pmatrix}, \tag{12}$$

with the differential and multiplication operators

$$L_\varepsilon := \varepsilon^2\partial_x^2 + 1 - 3u^h(x)^2, \quad S := \text{diag}(\partial_x^2 - 1, D^2\partial_x^2 - 1), \\ A := (-\alpha - \beta), \quad B := \begin{pmatrix} 1 \\ 1 \end{pmatrix}.$$

We have $L_\varepsilon : H^2 \subset L^2 \rightarrow L^2, S : H^2 \times H^2 \subset L^2 \times L^2 \rightarrow L^2 \times L^2$, and $A : L^2 \times L^2 \rightarrow L^2, B : L^2 \rightarrow L^2 \times L^2$, where we suppressed the spatial domain \mathbb{R} in each case.

Lemma 1 (Spectrum of the operator L_ε) *The operator $L_\varepsilon : H^2 \subset L^2 \rightarrow L^2$ is self-adjoint with maximal eigenvalue*

$$\mu_\varepsilon = \varepsilon^2\tilde{\mu}_\varepsilon = \mathcal{O}(\varepsilon^2), \text{ where } \lim_{\varepsilon \rightarrow 0} \tilde{\mu}_\varepsilon = \tilde{\mu}_0 = \frac{3\sqrt{2}}{2} \left(\alpha + \frac{\beta}{D} \right),$$

and with corresponding eigenfunction $\phi = \phi_\varepsilon = \varepsilon^{-1}\phi_0(x/\varepsilon) + \mathcal{O}(\varepsilon), \phi_0 = (\sqrt{2}/2)\text{sech}^2(\cdot/\sqrt{2})$.

Proof See Appendix B. □

Consequently, we have the orthogonal splitting $L^2 = \text{span}(\phi) \oplus X, X = \text{range}(L_\varepsilon)$ so that $L_\varepsilon^{-1} : X \rightarrow X$ is bounded. The splitting is associated with the projections $P = \langle \cdot, \phi \rangle \phi$, i.e., $\ker(P) = X, \text{range}(P) = \text{span}(\phi)$ and the complementary projection $Q = \text{Id} - P$. Hence, the ‘partial’ resolvent

$$T_\varepsilon := L_\varepsilon^{-1}Q : L^2 \rightarrow L^2 \tag{13}$$

is bounded for each $\varepsilon > 0$. Furthermore, we have that $S^{-1} : L^2 \times L^2 \rightarrow L^2 \times L^2$ is bounded and independent of ε .

Let us now represent $\tilde{\Psi}_u \in L^2$ according to the splitting induced by L_ε , that is,

$$\tilde{\Psi}_u = d\phi + Q[\tilde{\Psi}_u]. \tag{14}$$

Hence, the construction of $\tilde{\Psi}_u$ amounts to finding d and $Q[\tilde{\Psi}_u]$. Then, (12) becomes

$$L_\varepsilon \tilde{\Psi}_u + \varepsilon A \tilde{\Psi}_{v,w} = \varepsilon^2 \Psi_u \implies d\mu_\varepsilon \phi + L_\varepsilon Q[\tilde{\Psi}_u] + \varepsilon A \tilde{\Psi}_{v,w} = \varepsilon^2 \Psi_u, \tag{15}$$

and

$$B \tilde{\Psi}_u + S \tilde{\Psi}_{v,w} = \Psi_{v,w} \implies dB\phi + BQ[\tilde{\Psi}_u] + S \tilde{\Psi}_{v,w} = \Psi_{v,w}. \tag{16}$$

Upon letting P and Q act on (15), we get

$$d\mu_\varepsilon \|\phi\|^2 = \langle \varepsilon^2 \Psi_u - \varepsilon A \tilde{\Psi}_{v,w}, \phi \rangle, \text{ and} \tag{17}$$

$$L_\varepsilon Q[\tilde{\Psi}_u] = Q[\varepsilon^2 \Psi_u - \varepsilon A \tilde{\Psi}_{v,w}]. \tag{18}$$

Using the definition of T_ε from (13), Eq. (18) can be rearranged to

$$Q[\tilde{\Psi}_u] = T_\varepsilon[\varepsilon^2 \Psi_u - \varepsilon A \tilde{\Psi}_{v,w}]. \tag{19}$$

Inserting back into (16) gives

$$dB\phi + BT_\varepsilon[\varepsilon^2 \Psi_u - \varepsilon A \tilde{\Psi}_{v,w}] + S \tilde{\Psi}_{v,w} = \Psi_{v,w}.$$

After rearranging, this can be written as the equation for $\tilde{\Psi}_{v,w}$

$$\mathcal{N}_\varepsilon \tilde{\Psi}_{v,w} := (S - \varepsilon BT_\varepsilon A) \tilde{\Psi}_{v,w} = \Psi_{v,w} - \varepsilon^2 BT_\varepsilon \Psi_u - dB\phi.$$

Since ε is small, \mathcal{N}_ε is invertible, see Lemma 2 below, and we get

$$\tilde{\Psi}_{v,w} = \mathcal{N}_\varepsilon^{-1}[\Psi_{v,w} - \varepsilon^2 BT_\varepsilon \Psi_u - dB\phi]. \tag{20}$$

Finally, we insert this expression into (17) to get, as solvability condition for the existence problem (11) of the second generalized eigenfunction $\tilde{\Psi}$, the equation

$$\begin{aligned} 0 &= \left\langle \varepsilon^2 \Psi_u - \varepsilon A \mathcal{N}_\varepsilon^{-1} \left[\begin{pmatrix} \hat{\tau} \Psi_v \\ \hat{\theta} \Psi_w \end{pmatrix} - \varepsilon^2 BT_\varepsilon \Psi_u - dB\phi \right], \phi \right\rangle - \varepsilon^2 d\tilde{\mu}_\varepsilon \|\phi\|^2 \\ &= \left\langle \varepsilon^2 \Psi_u - \varepsilon A \mathcal{N}_\varepsilon^{-1} \left[\begin{pmatrix} \hat{\tau} \Psi_v \\ \hat{\theta} \Psi_w \end{pmatrix} - \varepsilon^2 BT_\varepsilon \Psi_u \right], \phi \right\rangle + dE, \end{aligned} \tag{21}$$

with $E = \langle \varepsilon A \mathcal{N}_\varepsilon^{-1} B\phi, \phi \rangle - \varepsilon^2 \tilde{\mu}_\varepsilon \|\phi\|^2$. If $E \neq 0$, one could always—for any parameter settings—satisfy this solvability condition by choosing d accordingly and thus obtain a second generalized eigenfunction. However, from the Evans function we know that a multiple zero eigenvalue requires adjustment of parameters according to

(8). Hence, it follows that $E = 0$ so that d remains unspecified, which is natural since (11) does not determine $\tilde{\Psi}$ uniquely; any multiple of Φ can be added to create another solution.

Upon dividing (21) by ε , we thus obtain the so-called SLEP-equation

$$0 = \left\langle \varepsilon \Psi_u - A \mathcal{N}_\varepsilon^{-1} \left[\begin{pmatrix} \hat{\tau} \Psi_v \\ \hat{\theta} \Psi_w \end{pmatrix} - \varepsilon^2 B T_\varepsilon \Psi_u \right], \phi \right\rangle. \tag{22}$$

The existence of $\tilde{\Psi}$ is now equivalent to solving (22), and $\tilde{\Psi}$ is then given by (14), (19) and (20) for an arbitrary scalar d . In order to characterize the solvability of (22), we conclude as follows. We first compute the leading order in ε and continuity as $\varepsilon \rightarrow 0$, which verifies that it coincides with the triple zero condition (8), and then use the implicit function theorem.

Lemma 2 *It holds true for $\varepsilon \rightarrow 0$ that $T_\varepsilon : L^2 \rightarrow L^2$ is uniformly bounded, with*

$$\left(T_\varepsilon + \frac{1}{2} \right) \rightarrow 0,$$

from $X \cap H^2$ to L^2 and

$$\mathcal{N}_\varepsilon^{-1} \rightarrow S^{-1} : L^2 \times L^2 \rightarrow H^2 \times H^2.$$

Proof First note that $T_\varepsilon = L_\varepsilon^{-1} Q$ is bounded on L^2 uniformly in ε since rescaling via $y = x/\varepsilon$, which does not change the operator norm ($\|u(\cdot)\|_2 = \sqrt{\varepsilon} \|u(\varepsilon \cdot)\|_2$), gives L_ε as $\partial_{yy} + a_\varepsilon(\varepsilon y)$ with $a_\varepsilon(x) = 1 - 3u^h(x)^2$ so $a_0(x) \rightarrow -2$ as $x \rightarrow \pm\infty$ (u^h being the u -component of the stationary front). Hence, the rescaled T_ε is bounded uniformly in ε . This implies the same for $\mathcal{N}_\varepsilon^{-1}$ so that $\mathcal{N}_\varepsilon^{-1} \rightarrow \mathcal{N}_0^{-1}$ as an operator on L^2 . Formally, $T_\varepsilon \rightarrow T_0 = a_0^{-1} \equiv -\frac{1}{2}$, which is however incorrect in the sense of operator converge on L^2 and this makes the proof a bit involved. Due to the uniform boundedness of T_ε on L^2 , we have $T_\varepsilon - a_0^{-1} : L^2 \rightarrow L^2$ uniformly bounded in $\varepsilon > 0$, so that convergence of $(T_\varepsilon - a_\varepsilon^{-1})v$ with $v \in L^2$ follows from consideration of a dense subset such as $v \in H^2$. We compute, using $T_\varepsilon^{-1} = L_\varepsilon$ on $X = \text{range}(T_\varepsilon)$ and that a_0^{-1} commutes,

$$\begin{aligned} T_\varepsilon - a_0^{-1} &= a_0^{-1} a_0 T_\varepsilon - a_0^{-1} T_\varepsilon T_\varepsilon^{-1} \\ &= a_0^{-1} T_\varepsilon (a_0 - (\varepsilon^2 \partial_{xx} + a_\varepsilon)) \\ &= a_0^{-1} T_\varepsilon (a_0 - a_\varepsilon) - \varepsilon^2 a_0^{-1} T_\varepsilon \partial_{xx}. \end{aligned}$$

Since $a_\varepsilon \rightarrow a_0$ in L^2 it follows that $(T_\varepsilon - a_0^{-1}) \rightarrow 0$ from $X \cap H^2$ to L^2 as required.

Furthermore, we have $\mathcal{N}_\varepsilon \rightarrow \mathcal{N}_0 = S : H^2 \times H^2 \rightarrow L^2 \times L^2$ and for the resolvent we even have $\mathcal{N}_\varepsilon^{-1} \rightarrow S^{-1} : L^2 \times L^2 \rightarrow H^2 \times H^2$ since $\mathcal{N}_\varepsilon^{-1} - S^{-1} = \varepsilon S^{-1} B T_\varepsilon A \mathcal{N}_\varepsilon^{-1}$ and $S^{-1} B T_\varepsilon A \mathcal{N}_\varepsilon^{-1} : L^2 \times L^2 \rightarrow L^2 \times L^2$ is uniformly bounded, so the claim follows from $S^{-1} : L^2 \times L^2 \rightarrow H^2 \times H^2$ being bounded and constant in ε . □

Equipped with this, we can compute the leading order of (22) based on the following observations: Since $\lim_{\varepsilon \rightarrow 0} \mathcal{N}_\varepsilon^{-1} = S^{-1}$ and ϕ_ε forms a Dirac sequence with limiting mass $\int_{\mathbb{R}} \phi_0 = 2$, we have $\langle f, \phi_\varepsilon \rangle \rightarrow 2f(0)$ for, e.g., bounded, integrable and uniformly continuous f . Regarding S^{-1} , we use $(D^2\partial_{xx} - 1)^{-1}f = G_{D^2} * f$ with Green’s function $G_{D^2}(y) = -\frac{1}{2D}, \exp(-|y|/D)$ for localized solutions. This immediately gives

$$\begin{aligned} \lim_{\varepsilon \rightarrow 0} \langle A\mathcal{N}_\varepsilon^{-1}f, \phi \rangle &= 2(AS^{-1}[f])(0) \\ &= -2\alpha(G_1 * f_1)(0) - 2\beta(G_{D^2} * f_2)(0). \end{aligned} \tag{23}$$

As to the leading order terms in (22), using the leading order computation of Ψ from Lemma 6 of Appendix A, we see that Ψ_u is bounded so that

$$\lim_{\varepsilon \rightarrow 0} \langle \varepsilon\Psi_u, \phi \rangle = 0,$$

and also

$$\lim_{\varepsilon \rightarrow 0} \langle \varepsilon^2 A\mathcal{N}_\varepsilon^{-1} [BT_\varepsilon\Psi_u], \phi \rangle = 0.$$

Hence, for the leading order analysis of the SLEP-equation (22) there is just one remaining term

$$\left\langle A\mathcal{N}_\varepsilon^{-1} \left[\begin{pmatrix} \hat{\tau}\Psi_v \\ \hat{\theta}\Psi_w \end{pmatrix} \right], \phi \right\rangle.$$

Finally, taking the explicit form of the leading order approximation of the v, w -components of Ψ , see Lemma 6 of Appendix A, for f_1, f_2 in (23)³ gives

$$\lim_{\varepsilon \rightarrow 0} \left\langle A\mathcal{N}_\varepsilon^{-1} \left[\begin{pmatrix} \hat{\tau}\Psi_v \\ \hat{\theta}\Psi_w \end{pmatrix} \right], \phi \right\rangle = -\frac{3}{4} \left(\alpha\hat{\tau}^2 + \frac{\beta}{D}\hat{\theta}^2 \right). \tag{24}$$

In order to finish the proof of Proposition 2, we show that (22) can be solved by an implicit function theorem: We seek an ε -dependent family of parameters for $0 \leq \varepsilon \ll 1$ such that (22) holds, which—in view of (24)—at $\varepsilon = 0$ reduces to $\kappa_2^0 = 0$, and this can readily be solved by adjusting parameters. For simplicity, we consider deviations from $K = \kappa_2^0$, i.e., $K(\varepsilon) = \kappa_2^0 + \mu(\varepsilon)$, with $\mu(0) = 0$ so $K(0) = \kappa_2^0$. Let $h(\mu, \varepsilon)$ denote the right-hand side of (22), i.e., we want to solve $h(\mu, \varepsilon) = 0$ for each $0 \leq \varepsilon \ll 1$ in terms of μ . Notably, h is continuously differentiable in μ for $0 \leq \varepsilon \ll 1$ and continuous in ε in this interval (this is pointwise for the operators) so there is continuous \tilde{h} such that

$$h(\mu, \varepsilon) = h(0, \varepsilon) + h_\mu(0, \varepsilon)\mu + \tilde{h}(\mu, \varepsilon)\mu^2 = 0.$$

³ This amounts to solving the exact same inhomogeneous ODEs as in (51) of Appendix A, whose solutions evaluated at $x = 0$ yield exactly (52).

From $K = \alpha \hat{\tau}^2 + \beta \hat{\theta}^2/D$, we have

$$\partial_K = \hat{\tau}^2 \partial_\alpha + (\hat{\theta}^2/D) \partial_\beta$$

so that

$$\begin{aligned} h_\mu(0, 0) &= \lim_{\varepsilon \rightarrow 0} h_\mu(0, \varepsilon) = \partial_K|_{K=\kappa_2^0} \lim_{\varepsilon \rightarrow 0} \left\langle AN_\varepsilon^{-1} \left[\begin{pmatrix} \hat{\tau} \Psi_v \\ \hat{\theta} \Psi_w \end{pmatrix} \right], \phi \right\rangle \\ &= \hat{\tau}^2 \left(-\frac{3}{4} \hat{\tau}^2 \right) + (\hat{\theta}^2/D) \left(-\frac{3}{4} \hat{\theta}^2/D \right), \end{aligned}$$

which is nonzero (strictly negative) since $\hat{\tau}, \hat{\theta} > 0$.

By continuity, $h_\mu(0, \varepsilon) \neq 0$ for $0 \leq \varepsilon \ll 1$ so that $h(\mu, \varepsilon) = 0$ is equivalent to

$$\mu = -h_\mu(0, \varepsilon)^{-1} (h(0, \varepsilon) + \tilde{h}(\mu, \varepsilon) \mu^2).$$

This can be solved by Banach’s fixed point theorem with continuous parameter since the contraction constant can be chosen uniform in $0 \leq \varepsilon \ll 1$, which yields the desired solution family $\mu = \mu(\varepsilon)$ satisfying $h(\mu(\varepsilon), \varepsilon) = 0$. Therefore, by local uniqueness of solutions, if $\alpha, \beta, \hat{\tau}, \hat{\theta}, D$ satisfy $h(\mu(\varepsilon), \varepsilon) = 0$ for small enough $\varepsilon = 0$ we can construct a generalized eigenfunction and also continue this, together with the parameters, uniquely in terms of ε to $\varepsilon = 0$.

This completes the proof of Proposition 2.

Remark 1 The above proof works exactly the same for the existence problem of the first generalized eigenfunction Ψ

$$\mathcal{L}\Psi = \varepsilon^2 \Phi,$$

where $\mathcal{L}\Phi = 0$. The SLEP equation (22) then becomes

$$0 = \left\langle \varepsilon^2 \Phi_u - \varepsilon AN_\varepsilon^{-1} \left[\begin{pmatrix} \hat{\tau} \Phi_v \\ \hat{\theta} \Phi_w \end{pmatrix} - \varepsilon^2 BT_\varepsilon \Phi_u \right], \phi \right\rangle. \tag{25}$$

Since by Lemma 5 of Appendix A we have that $\Phi_u = \varepsilon^{-1} \phi_0(\cdot/\varepsilon) + \phi_1$ for a bounded exponentially localized ϕ_1 , we have

$$\lim_{\varepsilon \rightarrow 0} \langle \varepsilon \Phi_u, \phi \rangle = \lim_{\varepsilon \rightarrow 0} \varepsilon^{-1} \langle \phi_0(\cdot/\varepsilon), \phi_0(\cdot/\varepsilon) \rangle = \|\phi_0\|_2^2 = \frac{2\sqrt{2}}{3}.$$

Moreover, for $f_1 = \hat{\tau}\Phi_v = \hat{\tau} \exp^{-|x|}$, $f_2 = \hat{\theta}\Phi_w = \hat{\theta} \exp^{-|x|/D}$ in (23) we compute $(G_1 * f_1)(0) = -\frac{\hat{\tau}}{2}$ and $(G_{D^2} * f_2)(0) = -\frac{\hat{\theta}}{2D}$. Therefore, (25) becomes

$$0 = \frac{2\sqrt{2}}{3} - \alpha\hat{\tau} - \beta\hat{\theta}/D = \kappa_1^0,$$

see (6), and which is precisely the leading order of (7) as expected.

3 Center Manifold Reduction Using the Triple Zero Eigenvalue as Organizing Center

Let us again write our original system (1) in the more concise form

$$M(\hat{\tau}, \hat{\theta})\partial_t Z = F(Z; \alpha, \beta, D), \tag{26}$$

with $M(\hat{\tau}, \hat{\theta})$ and $F(Z; \alpha, \beta, D)$ as in (4). For the center manifold reduction, we make an ansatz adjusted to the translation invariance of our problem,

$$Z(x, t) = Z^{\text{sf}}(x - a(t)) + \tilde{R}(x - a(t), t), \tag{27}$$

with $Z^{\text{sf}} = (u^h, v^h, w^h)$ the stationary front (whose leading order was given in (3)), so that a is the position of the pseudo-front solutions.

Theorem 1 *Let $\varepsilon > 0$ be sufficiently small and let the system parameters be a perturbation of (8). Then, in a ‘tubular’ neighborhood of the spatial translates of Z^{sf} in $(L^2(\mathbb{R}))^3$ system (26) possesses an exponentially attracting three-dimensional center manifold, and the reduced vector field for the center manifold variables (a, c, \tilde{c}) can be cast as follows. The position a satisfies $\dot{a} = \varepsilon^2 c$, which identifies $\varepsilon^2 c$ as the velocity, and it is governed by the planar ordinary differential equations (ODE)*

$$\begin{pmatrix} \dot{a} \\ \dot{\tilde{c}} \end{pmatrix} = \varepsilon^2 \begin{pmatrix} 0 & 1 \\ 0 & 0 \end{pmatrix} \begin{pmatrix} a \\ \tilde{c} \end{pmatrix} + \begin{pmatrix} 0 \\ \varepsilon^2 G(c, \tilde{c}) \end{pmatrix} = \begin{pmatrix} \varepsilon^2 \tilde{c} \\ \varepsilon^2 G(c, \tilde{c}) \end{pmatrix}, \tag{28}$$

where G is smooth in its arguments and the parameters, and possesses the symmetry $(c, \tilde{c}) \rightarrow -(c, \tilde{c})$. In particular, $G(c, 0) = 0$ if and only if $T_\Gamma(c) = 0$ to any order, where T_Γ is the Taylor expansion of Γ with $\gamma = 0$ at $c = 0$.

In the following, we first prove this reduction and then analyze the reduced dynamics.

3.1 Center Manifold Reduction (Proof of Theorem 1)

Setting $\eta = x - a(t)$ and substitution of (27) into (26) gives (suppressing parameters)

$$-\dot{a}(t)M(\Phi(\eta) + \partial_\eta \tilde{R}(\eta, t)) + M\partial_t \tilde{R}(\eta, t) = F(Z^{\text{sf}}(\eta) + \tilde{R}(\eta, t)),$$

which can be written as

$$-\dot{a}(t) (\Phi(\eta) + \partial_\eta \tilde{R}(\eta, t)) + \partial_t \tilde{R} = \mathcal{L}\tilde{R} + \mathcal{N}(\tilde{R}),$$

with \mathcal{L}, \mathcal{N} as follows. By assumption, we have $\hat{\tau} = \hat{\tau}_0 + \check{\tau}, \hat{\theta} = \hat{\theta}_0 + \check{\theta}$ (and likewise for α, β, D), where subindex zero denotes the parameters values of a parameter set at which (8) holds. Now, $\mathcal{L} := M(\hat{\tau}_0, \hat{\theta}_0)^{-1} \partial_Z F(Z^{\text{sf}})$, which, after some simplifications, yields

$$\mathcal{N}(\tilde{R}) = \begin{pmatrix} 0 & 0 & 0 \\ 0 & -\frac{\check{\tau}}{\hat{\tau}_0 + \check{\tau}} & 0 \\ 0 & 0 & -\frac{\check{\theta}}{\hat{\theta}_0 + \check{\theta}} \end{pmatrix} M(\hat{\tau}_0, \hat{\theta}_0)^{-1} \partial_Z F(Z^{\text{sf}}) \tilde{R} - \begin{pmatrix} 3(Z^{\text{sf}})^u (\tilde{R}^u)^2 + (\tilde{R}^u)^3 \\ 0 \\ 0 \end{pmatrix}.$$

Using the Jordan block structure of \mathcal{L} (as stated in Proposition 2), we refine the ansatz to

$$\tilde{R}(x - a(t), t) = b(t)\Psi(x - a(t)) + \tilde{b}(t)\tilde{\Psi}(x - a(t)) + R(x - a(t), t),$$

where R is L^2 -orthogonal to the adjoint generalized kernel spanned by $\Phi^*, \Psi^*, \tilde{\Psi}^*$. Hence,

$$Z(x, t) = Z^{\text{sf}}(x - a(t)) + b(t)\Psi(x - a(t)) + \tilde{b}(t)\tilde{\Psi}(x - a(t)) + R(x - a(t), t),$$

and, suppressing the dependence of $\Psi, \tilde{\Psi}$ and R on η ,

$$\begin{aligned} &-\dot{a}(t) (\Phi + b(t)\Psi' + \tilde{b}(t)\tilde{\Psi}' + \partial_\eta R(t)) + \dot{b}(t)\Psi + \dot{\tilde{b}}(t)\tilde{\Psi} + \partial_t R(t) \\ &= \varepsilon^2 b(t)\Phi + \varepsilon^2 \tilde{b}(t)\Psi + \mathcal{L}R(t) + \mathcal{N}(b(t)\Psi + \tilde{b}(t)\tilde{\Psi} + R(t)). \end{aligned} \tag{29}$$

Recall that Z^{sf} is odd, so $\Phi = (Z^{\text{sf}})'$ is even, and $\Psi, \tilde{\Psi}, \Phi^*, \Psi^*, \tilde{\Psi}^*$ are all also even, such that their derivatives are odd, and, hence,

$$\langle \Psi', \Phi^* \rangle = \langle \tilde{\Psi}', \Phi^* \rangle = \langle \Psi', \Psi^* \rangle = \langle \tilde{\Psi}', \Psi^* \rangle = \langle \Psi', \tilde{\Psi}^* \rangle = \langle \tilde{\Psi}', \tilde{\Psi}^* \rangle = 0.$$

Executing the projections on (29) (and again suppressing parameter dependence) then gives the equations on the generalized kernel as

$$\begin{pmatrix} d_1 \\ d_2 \\ d_3 \end{pmatrix} \dot{a} + A \begin{pmatrix} \dot{a} \\ \dot{b} \\ \dot{\tilde{b}} \end{pmatrix} = \begin{pmatrix} 0 & p_1 & p_2 \\ 0 & 0 & p_1 \\ 0 & 0 & 0 \end{pmatrix} \begin{pmatrix} a \\ \varepsilon^2 b \\ \varepsilon^2 \tilde{b} \end{pmatrix} + \begin{pmatrix} \langle \mathcal{N}[b\Psi + \tilde{b}\tilde{\Psi} + R], \tilde{\Psi}^* \rangle \\ \langle \mathcal{N}[b\Psi + \tilde{b}\tilde{\Psi} + R], \Psi^* \rangle \\ \langle \mathcal{N}[b\Psi + \tilde{b}\tilde{\Psi} + R], \Phi^* \rangle \end{pmatrix},$$

with

$$A := \begin{pmatrix} p_1 & p_2 & p_3 \\ 0 & p_1 & p_2 \\ 0 & 0 & p_1 \end{pmatrix}, \quad d_1 := -\langle \partial_\eta R, \tilde{\Psi}^* \rangle, \quad d_2 := -\langle \partial_\eta R, \Psi^* \rangle, \quad d_3 := -\langle \partial_\eta R, \Phi^* \rangle,$$

and p_1, p_2, p_3 as in (10) of Proposition 2. Note that $d_1, d_2, d_3 \rightarrow 0$ as $R \rightarrow 0$ by integration by parts; in particular $|d_1| < 1$ in the range we consider due to the ansatz (27) from the tubular vicinity of Z^{sf} .

Multiplying the last equation by

$$A^{-1} = \begin{pmatrix} 1/p_1 & -p_2/p_1^2 & (p_2^2 - p_1 p_3)/p_1^3 \\ 0 & 1/p_1 & -p_2/p_1^2 \\ 0 & 0 & 1/p_1 \end{pmatrix}$$

gives the first form of the reduced system

$$\dot{a} \begin{pmatrix} q_1 \\ q_2 \\ q_3 \end{pmatrix} + \begin{pmatrix} \dot{a} \\ \dot{b} \\ \dot{\tilde{b}} \end{pmatrix} = \begin{pmatrix} 0 & 1 & 0 \\ 0 & 0 & 1 \\ 0 & 0 & 0 \end{pmatrix} \begin{pmatrix} a \\ \varepsilon^2 b \\ \varepsilon^2 \tilde{b} \end{pmatrix} + \begin{pmatrix} N_1[b, \tilde{b}, R] \\ N_2[b, \tilde{b}, R] \\ N_3[b, \tilde{b}, R] \end{pmatrix}, \tag{30}$$

where

$$q_1 := \frac{d_1}{p_1} - \frac{d_2 p_2}{p_1^2} + d_3 \frac{p_2^2 - p_1 p_3}{p_1^3}, \quad q_2 := \frac{d_2}{p_1} - \frac{d_3 p_2}{p_1^2}, \quad q_3 := \frac{d_3}{p_1},$$

and

$$\begin{pmatrix} N_1[b, \tilde{b}, R] \\ N_2[b, \tilde{b}, R] \\ N_3[b, \tilde{b}, R] \end{pmatrix} := A^{-1} \begin{pmatrix} \langle \mathcal{N}[b\Psi + \tilde{b}\tilde{\Psi} + R], \tilde{\Psi}^* \rangle \\ \langle \mathcal{N}[b\Psi + \tilde{b}\tilde{\Psi} + R], \Psi^* \rangle \\ \langle \mathcal{N}[b\Psi + \tilde{b}\tilde{\Psi} + R], \Phi^* \rangle \end{pmatrix}.$$

Observe now that the right-hand side of these equations does not depend explicitly on a . In particular, using the rescaling $(\underline{b}, \underline{\tilde{b}}) = (b/(q_1 + 1), \tilde{b}/(q_1 + 1))$ and denoting

$$\begin{aligned} \underline{N}_j[b, \tilde{b}, R] &:= N_j[(q_1 + 1)\underline{b}, (q_1 + 1)\underline{\tilde{b}}, R] \\ g(\underline{b}, \underline{\tilde{b}}, R) &:= \varepsilon^2 \underline{b} + \underline{N}_1[b, \tilde{b}, R]/(q_1 + 1), \end{aligned}$$

we can rewrite the system (30) as

$$\begin{aligned} \dot{a} &= \varepsilon^2 \underline{b} + \underline{N}_1[b, \tilde{b}, R]/(q_1 + 1), \\ \begin{pmatrix} \dot{\underline{b}} \\ \dot{\underline{\tilde{b}}} \end{pmatrix} &= \begin{pmatrix} 0 & 1 \\ 0 & 0 \end{pmatrix} \begin{pmatrix} \varepsilon^2 \underline{b} \\ \varepsilon^2 \underline{\tilde{b}} \end{pmatrix} + \begin{pmatrix} \underline{N}_2[b, \tilde{b}, R] - q_2 g(\underline{b}, \underline{\tilde{b}}, R) \\ \underline{N}_3[b, \tilde{b}, R] - q_3 g(\underline{b}, \underline{\tilde{b}}, R) \end{pmatrix}. \end{aligned}$$

The spectral properties noted in Proposition 2, the semi-linear problem structure and smoothness of the nonlinearity imply the existence of an exponentially attracting center

manifold for $0 < \varepsilon \ll 1$ (see, e.g., Haragus and Iooss 2011, Thm. 3.22). This means $R = H(\underline{b}, \tilde{b})$, with smooth function H independent of a since the right-hand side is independent of a [cf. Krupa (1990), and Sandstede et al. (1997) for the present case of a non-compact group; see also Haragus and Iooss 2011, Thm 3.19]. Hence, we get the reduced system

$$\begin{cases} \dot{a} = \varepsilon^2 \underline{b} + \varepsilon^2 F_1[\underline{b}, \tilde{b}], \\ \dot{\underline{b}} = \varepsilon^2 \tilde{b} + \varepsilon^2 F_2[\underline{b}, \tilde{b}], \\ \dot{\tilde{b}} = \varepsilon^2 F_3[\underline{b}, \tilde{b}], \end{cases} \tag{31}$$

with $F_1[\underline{b}, \tilde{b}] = \varepsilon^{-2} N_1[\underline{b}, \tilde{b}, H(\underline{b}, \tilde{b})]/(1+q_1)$, $F_2[\underline{b}, \tilde{b}] = \varepsilon^{-2} (N_2[\underline{b}, \tilde{b}, H(\underline{b}, \tilde{b})] - q_2 g(\underline{b}, \tilde{b}, H(\underline{b}, \tilde{b})))$, and $F_3[\underline{b}, \tilde{b}] = \varepsilon^{-2} (N_3[\underline{b}, \tilde{b}, H(\underline{b}, \tilde{b})] - q_3 g(\underline{b}, \tilde{b}, H(\underline{b}, \tilde{b})))$, and where the seemingly singular scaling of F_j will be justified in the next section. We will not explicitly compute F_j in terms of projections and the expansion of the center manifold, but rather perform another transformation that connects the coordinates on the center manifold with the velocity.

Lemma 3 *There exists a near-identity change of variables $(\underline{b}, \tilde{b}) \mapsto (c, \tilde{c})$ such that (31) becomes*

$$\begin{aligned} \dot{a} &= \varepsilon^2 c, \\ \begin{pmatrix} \dot{c} \\ \dot{\tilde{c}} \end{pmatrix} &= \varepsilon^2 \begin{pmatrix} 0 & 1 \\ 0 & 0 \end{pmatrix} \begin{pmatrix} c \\ \tilde{c} \end{pmatrix} + \begin{pmatrix} 0 \\ \varepsilon^2 G(c, \tilde{c}) \end{pmatrix}. \end{aligned}$$

Proof We first make the near-identity change of variables $c := \underline{b} + F_1[\underline{b}, \tilde{b}]$, which can be inverted locally to $\underline{b} = \mathcal{A}_1(c, \tilde{b})$. So $\dot{a} = \varepsilon^2 c$, and taking a derivative gives

$$\dot{c} = \varepsilon^2 \tilde{b} + \varepsilon^2 \underline{F}_2[c, \tilde{b}]$$

with

$$\begin{aligned} \underline{F}_2[c, \tilde{b}] &= F_2[\mathcal{A}_1(c, \tilde{b}), \tilde{b}] + \partial_1 F_1[\mathcal{A}_1(c, \tilde{b}), \tilde{b}](\tilde{b} + F_2[\mathcal{A}_1(c, \tilde{b}), \tilde{b}]) \\ &\quad + \partial_2 F_1[\mathcal{A}_1(c, \tilde{b}), \tilde{b}] F_3[\mathcal{A}_1(c, \tilde{b}), \tilde{b}]. \end{aligned}$$

A further near-identity change of variables by $\tilde{c} := \tilde{b} + F_2[c, \tilde{b}]$ (again locally invertible to $\tilde{b} = \mathcal{A}_2(c, \tilde{c})$) gives $\dot{c} = \varepsilon^2 \tilde{c}$. Finally, taking a derivative as before we obtain

$$\dot{\tilde{c}} = \varepsilon^2 G(c, \tilde{c}),$$

where G can be specified in terms of $\underline{F}_2, F_1, F_2, F_3$ analogous to the previous step, though we make no direct use of this. □

The advantage of this reformulation is that equilibria in these coordinates, $G(c, 0) = 0$, are traveling fronts with this c -value as its velocity to any expansion order. Regarding symmetry, the reflection symmetries of (26) $x \rightarrow -x$ and $Z \rightarrow -Z$ imply that H

can be chosen to respect this in the reduced coordinates, which gives the claimed symmetry with respect to the reflection

$$(\eta, a, c, \tilde{c}) \rightarrow -(\eta, a, c, \tilde{c}).$$

This completes the proof of Theorem 1.

3.2 Dynamics of the Reduced System on the Center Manifold

Since the planar ODE for the velocity c has the form (28), one can already anticipate a Bogdanov–Takens-type bifurcation scenario. The type of unfolding is determined by the degeneracies in the expansion of $G(c, \tilde{c})$ in (28). That is,

$$G(c, \tilde{c})|_{\varepsilon=0} = g_1 c + g_3 c^3 + \sigma_1 c^5 + \tilde{c}(g_2 + g_4 c^2 + \sigma_2 c^4) + O(\tilde{c}^2) + h.o.t., \quad (32)$$

where g_j are functions of the system parameters. We will later select system parameters to unfold the bifurcation, and for now denote by μ an abstract selection of system parameters, so that $g_j = g_j(\mu)$ and $\mu = 0$ is the bifurcation point.

Definition 1 Concerning the possible degeneracies we say that we have a

- *symmetric Bogdanov–Takens (SBT)* iff $g_1|_{\mu=0} = g_2|_{\mu=0} = 0$ and $g_3 g_4|_{\mu=0} \neq 0$, see Fig. 3;
- *symmetric Bogdanov–Takens with butterfly imprint (SBTB)* iff $g_1|_{\mu=0} = g_2|_{\mu=0} = g_3|_{\mu=0} = 0$ and $g_4|_{\mu=0} \neq 0$; and
- *symmetric Bogdanov–Takens with degeneracy (SBTD)* iff $g_1|_{\mu=0} = g_2|_{\mu=0} = g_4|_{\mu=0} = 0$ and $g_3|_{\mu=0} \neq 0$.

A normal form for these cases, as well as the additional option of $g_1|_{\mu=0} = g_2|_{\mu=0} = g_3|_{\mu=0} = g_4|_{\mu=0}$, has been derived in Knobloch (1986). This normal form is, in the slow time scale $\tau = \varepsilon^{-2} d/dt$, given by

$$\begin{cases} \underline{c}' = \tilde{c} \\ \underline{\tilde{c}}' = \underline{g}_1 \underline{c} + \underline{g}_3 \underline{c}^3 + \underline{\sigma}_1 \underline{c}^5 + \tilde{c} \left(\underline{g}_2 + \underline{g}_4 \underline{c}^2 + \underline{\sigma}_2 \underline{c}^4 \right), \end{cases}$$

where the underscores emphasize that, in general, an additional coordinate change is required to reach this normal form. However, in the SBT case this is not needed and we can also ignore $\underline{\sigma}_1$ and $\underline{\sigma}_2$. In contrast, in the SBTB case the additional coordinate change depends on the coefficient $\partial_c \partial_{\tilde{c}}^2 G(0, 0)$, see Knobloch (1986). Since our approach does not provide access to compute $\partial_c \partial_{\tilde{c}}^2 G(0, 0)$, it does not allow to rigorously unfold this case.

In this paper, we focus on the SBT case, so that two parameters $\mu = (\mu_1, \mu_2)$ suffice, and follow the analysis in Carr (1981) to check the relevant terms in the right-hand side G in (28) directly, by explicitly computing some of its derivatives. As alluded to, in these computations we exploit the analytic information on the (leading order) existence condition and critical eigenvalues for uniformly traveling fronts, i.e., for the

fixed points (28). Since all coefficients are continuous at $\varepsilon = 0$, it suffices to focus on the leading order at $\varepsilon = 0$. For convenience, we first summarize the information needed from the existence and stability analysis, see also Chirilus-Bruckner et al. (2015).

The leading order in ε of the Evans function arising from the stability analysis of uniformly traveling fronts has been determined in Chirilus-Bruckner et al. (2015) to be

$$\mathcal{D}(\hat{\lambda}, c) = -\frac{\sqrt{2}}{6}\hat{\lambda} + \alpha\tilde{\mathcal{D}}(\hat{\lambda}, c\hat{\tau}, \hat{\tau}) + \frac{\beta}{D}\tilde{\mathcal{D}}\left(\hat{\lambda}, c\frac{\hat{\theta}}{D}, \hat{\theta}\right) = 0,$$

with

$$\tilde{\mathcal{D}}(\hat{\lambda}, \rho_1, \rho_2) = \left(\frac{1}{\sqrt{\rho_1^2 + 4}} - \frac{1}{\sqrt{\rho_1^2 + 4(\hat{\lambda}\rho_2 + 1)}} \right).$$

Lemma 4 *Let $\kappa_1^0, \kappa_2^0, \kappa_3^0$ be as in (6). Then, the Taylor expansion in $c = 0$ of the leading order existence condition from (2) for uniformly traveling fronts with velocity $\varepsilon^2 c$ for $\gamma = 0$ is given by*

$$T_\Gamma(c) = \frac{1}{2}\kappa_1^0 c - \frac{1}{16}\kappa_3^0 c^3 + kc^5 + O(c^7), \tag{33}$$

where $k = \frac{3}{256} \left(\alpha\hat{\tau}^5 + \beta\frac{\hat{\theta}^5}{D^5} \right)$ does not vanish if $\kappa_1^0 = \kappa_3^0 = 0$. Furthermore, the leading order of the Evans function⁴ arising from the stability analysis of uniformly traveling fronts (with translational eigenvalue factored out) has the form

$$\mathcal{E}(\hat{\lambda}, c) = \frac{\mathcal{D}(\hat{\lambda}, c)}{\hat{\lambda}} = a_0(c) + a_1(c)\hat{\lambda} + a_2(c)\hat{\lambda}^2 + a_3(c)\hat{\lambda}^3 + O(\hat{\lambda}^4)$$

and is an even function of c with expansions of the coefficients given by $a_i = \sum_{j \geq 0} a_{2j,i} c^{2j}$ with

$$\begin{cases} a_{00} = \frac{1}{4}\kappa_1^0, & a_{20} = -\frac{3}{32}\kappa_3^0, & a_{01} = -\frac{3}{16}\kappa_2^0, & a_{21} = \frac{15}{128} \left(\alpha\hat{\tau}^4 + \frac{\beta}{D^3}\hat{\theta}^4 \right), \\ a_{02} = \frac{5}{32} \left(\alpha\hat{\tau}^3 + \frac{\beta}{D}\hat{\theta}^3 \right), & a_{03} = -\frac{35}{256} \left(\alpha\hat{\tau}^4 + \frac{\beta}{D}\hat{\theta}^4 \right). \end{cases} \tag{34}$$

⁴ Note that the Evans function and \mathcal{E} are meaningful only for choices of c and system parameters such that a traveling front with velocity c exists.

In the following, we will make use of the Taylor coefficients a_{ij} of the Evans function to derive expressions for the coefficients of the reduced system on the center manifold and discuss the unfolding of its bifurcation structure. Hence,

$$a_{ij} = a_{ij}(\mu), \tag{35}$$

where $\mu = (\mu_1, \mu_2)$ is some choice of unfolding parameters.

Proof of Lemma 4 A straightforward computation yields the Taylor expansion of the existence condition (2) (with $\gamma = 0$). In order to verify that $k \neq 0$ at $\kappa_1^0 = \kappa_3^0 = 0$, we can use that $\kappa_1^0 = \kappa_3^0 = 0$ can be expressed as

$$\alpha = -\frac{2\sqrt{2}}{3} \frac{\hat{\theta}^2}{\hat{\tau}(D^2\hat{\tau}^2 - \hat{\theta}^2)}, \quad \beta = \frac{2\sqrt{2}}{3} \frac{D^3\hat{\tau}^2}{\hat{\theta}(D^2\hat{\tau}^2 - \hat{\theta}^2)},$$

with automatically nonzero denominator at $\kappa_1^0 = \kappa_3^0 = 0$. This gives

$$k|_{\kappa_1^0=\kappa_3^0=0} = -\frac{\sqrt{2}}{128} \hat{\tau}^2 \left(\frac{\hat{\theta}}{D}\right)^2 \neq 0.$$

Another straightforward calculation gives

$$\begin{aligned} a_0(c) &= -\frac{\sqrt{2}}{6} + 2\alpha\hat{\tau}(\mathcal{F}(c\hat{\tau}))^3 + 2\frac{\beta}{D}\hat{\theta}(\mathcal{F}(c\hat{\theta}/D))^3, \\ a_1(c) &= -6\alpha\hat{\tau}^2(\mathcal{F}(c\hat{\tau}))^5 - 6\frac{\beta}{D}\hat{\theta}^2(\mathcal{F}(c\hat{\theta}/D))^5, \\ a_2(c) &= 20\alpha\hat{\tau}^3(\mathcal{F}(c\hat{\tau}))^7 + 20\frac{\beta}{D}\hat{\theta}^3(\mathcal{F}(c\hat{\theta}/D))^7, \\ a_3(c) &= -70\alpha\hat{\tau}^4(\mathcal{F}(c\hat{\tau}))^9 - 70\frac{\beta}{D}\hat{\theta}^4(\mathcal{F}(c\hat{\theta}/D))^9, \end{aligned}$$

with $\mathcal{F}(\rho_1) = (\rho_1^2 + 4)^{-1/2}$. Further direct computations yield the claimed Taylor expansions. □

3.2.1 Unfolding of the Codimension Two Case

Throughout this section, we denote by $\mu = (\mu_1, \mu_2)$ any choice of parameters in (1) with $(\kappa_1^0, \kappa_2^0)|_{\mu=0} = 0$, and denote with ∇_μ the gradient with respect to μ . The following proposition allows us to identify and unfold the SBT case.

Proposition 3 *The reduced system on the center manifold (28) has, to leading order in ε , the form*

$$\begin{cases} \dot{c} = \varepsilon^2 \tilde{c} \\ \dot{\tilde{c}} = \varepsilon^2 G(c, \tilde{c}, \mu) = \varepsilon^2 (G_1(c, \mu) + \tilde{c}G_2(c, \mu)) + o(\varepsilon^2), \end{cases}$$

where

$$\begin{aligned} G_1(c, \mu) &= [g_{10} + g_{11} \cdot \mu]c + g_{30}c^3 + h.o.t., \quad \text{and} \\ G_2(c, 0, \mu) &= g_{20} + g_{21} \cdot \mu + g_{40}c^2 + h.o.t., \end{aligned} \tag{36}$$

with $g_{j0} \in \mathbb{R}$, $g_{j1} \in \mathbb{R}^2$ (and, hence, linear functions $g_{j1} \cdot \mu$). Moreover, with a_{ij} from (34) and the notation from (35),

$$g_{10} = 0, \quad g_{20} = 0, \quad g_{30} = -\frac{1}{3} \frac{a_{20}(0)}{a_{02}(0)}, \quad g_{40} = -\frac{1}{a_{02}(0)} \left(a_{21}(0) - \frac{a_{20}(0)a_{03}(0)}{a_{02}(0)} \right),$$

that is, the linear part is, as expected, a Jordan block of length two at the organizing center, and

$$g_{11} = -\frac{\nabla_{\mu} a_{00}(0)}{a_{02}(0)}, \quad g_{21} = -\frac{1}{a_{02}(0)} \left[\nabla_{\mu} a_{01}(0) - \frac{\nabla_{\mu} a_{00}(0)a_{03}(0)}{a_{02}(0)} \right],$$

Corollary 1 *The coefficients g_{ij} from Proposition 3 satisfy*

$$g_{11} = \frac{6\sqrt{2}}{5\hat{\tau}\hat{\theta}} \left(\nabla_{\mu} \kappa_1^0 \right) \Big|_{\mu=0}, \tag{37}$$

$$g_{21} = -\frac{3}{5\sqrt{2}\hat{\tau}\hat{\theta}} \left(3\nabla_{\mu} \kappa_2^0 - \frac{7}{2}(\hat{\tau} + \hat{\theta})\nabla_{\mu} \kappa_1^0 \right) \Big|_{\mu=0}, \tag{38}$$

as well as

$$\begin{aligned} g_{30} &= -\frac{3}{20\sqrt{2}} \left(\frac{\kappa_3^0}{\hat{\tau}\hat{\theta}} \right) \Big|_{\mu=0} = \frac{1}{5} \frac{D^2\hat{\tau} - \hat{\theta}}{D^2(\hat{\tau} - \hat{\theta})} \Big|_{\mu=0}, \\ g_{40} &= -\frac{3}{40} \frac{3(D^2\hat{\tau}^2 - \hat{\theta}^2) + 7\hat{\tau}\hat{\theta}(1 - D^2)}{D^2(\hat{\tau} - \hat{\theta})} \Big|_{\mu=0}. \end{aligned}$$

In particular, $g_{30} = 0$ is equivalent to $\kappa_3^0|_{\mu=0} = 0$ and in this case $g_{40} = -\frac{3}{4}\hat{\tau} < 0$. Conversely, if $g_{40} = 0$ then $7\hat{\tau} > 3\hat{\theta}$ and $g_{30} = \frac{2\hat{\tau}}{7\hat{\tau} - 3\hat{\theta}} > 0$. Moreover, if $g_{30} < 0$ then $g_{40} < 0$.

Remark 2 The fact that $g_{30} = g_{40} = 0$ is not possible implies that the degeneracies of higher order than the SBT case are either the SBTB case or the SBTB case, see Definition 1.

Proof of Proposition 3 and Corollary 1 Since eigenvalues are invariant under coordinate changes, the eigenvalues of the linearization of (28) in equilibria coincide (in the sense of Taylor expansions) with the two small eigenvalues of the operator \mathcal{L} . Recall only these eigenvalues (and the fixed zero eigenvalue) of \mathcal{L} are close to the imaginary axis and satisfy $\lambda = \varepsilon^2\hat{\lambda}$, $\hat{\lambda} = \mathcal{O}(1)$. From this, we infer that $G = \mathcal{O}(1)$ with respect

to ε and also the two small eigenvalues $\hat{\lambda}_j^\varepsilon, j = 1, 2$, coincide with the eigenvalues of the linearization of (28) in equilibria. All quantities are at least continuous in ε at $\varepsilon = 0$, and we discuss the leading order next. Since fixed points of (28) are roots of $G(c, 0; \mu) = 0$, for some functions G_1, G_2 we have

$$G(c, \tilde{c}; \mu)|_{\varepsilon=0} = G_1(c; \mu) + \tilde{c}G_2(c, \tilde{c}; \mu),$$

where G_1 has the same zeros as T_Γ from (33). Linearizing the resulting system (in slow time) and evaluating at $\tilde{c} = 0$ gives the matrix

$$\begin{pmatrix} 0 & 1 \\ \partial_c G_1(c; \mu) & G_2(c, 0; \mu) \end{pmatrix},$$

whose characteristic equation

$$\hat{\lambda}^2 - G_2(c, 0; \mu)\hat{\lambda} - \partial_c G_1(c; \mu) = 0, \tag{39}$$

has the same roots as the (reduced) Evans function \mathcal{E} (in the sense of expansion). Precisely, two of these roots vanish at the SBT point $\kappa_1^0 = \kappa_2^0 = 0$ and \mathcal{E} is analytic. The Weierstrass preparation theorem, cf. e.g., Chow and Hale (1982), thus yields

$$\mathcal{E}(\hat{\lambda}, c; \mu) = \left(\hat{\lambda}^2 + \tilde{a}_1(c, \mu)\hat{\lambda} + \tilde{a}_0(c, \mu) \right) \tilde{\mathcal{E}}(\hat{\lambda}, c; \mu), \tag{40}$$

for unique \tilde{a}_0, \tilde{a}_1 and non-vanishing $\tilde{\mathcal{E}}$, all being holomorphic in c and system parameters in a neighborhood of the SBT point. Comparing (39) and (40) implies that

$$\mathcal{T}_{c,\mu}(-G_2) = \mathcal{T}_{c,\mu}(\tilde{a}_1), \quad \mathcal{T}_{c,\mu}(-\partial_c G_1) = \mathcal{T}_{c,\mu}(\tilde{a}_0), \tag{41}$$

that is, the Taylor expansions (including c and parameters) of $-\tilde{a}_1$ and $G_2(\cdot, 0)$, as well as $-\tilde{a}_0$ and $\partial_c G_1(\cdot)$ coincide, respectively. Since we know the Taylor expansion of \mathcal{E} from Lemma 4, we can employ a two-step procedure to derive the formulas for g_{ij} in (36):

Step 1 Compute the unknown \tilde{a}_j recursively from

$$\begin{aligned} \mathcal{E}(\hat{\lambda}, c; \mu) &= (\hat{\lambda}^2 + \tilde{a}_1(c, \mu)\hat{\lambda} + \tilde{a}_0(c, \mu))\tilde{\mathcal{E}}(\hat{\lambda}, c; \mu) \\ &= a_0(c, \mu) + a_1(c, \mu)\lambda + a_2(c, \mu)\lambda^2 + a_3(c, \mu)\lambda^3 + \dots, \end{aligned}$$

where the a_j 's are given in Lemma 4.

Step 2 Use (41) to determine the expressions for the g_{ij} .

Let us now turn our attention to the recursion. By analyticity,

$$\tilde{\mathcal{E}}(\hat{\lambda}, c; \mu) = \tilde{e}_0(c, \mu) + \tilde{e}_1(c, \mu)\lambda + \tilde{e}_2(c, \mu)\lambda^2 + \tilde{e}_3(c, \mu)\lambda^3 + \dots$$

and therefore

$$\begin{aligned} \mathcal{E}(\hat{\lambda}, c; \mu) &= (\hat{\lambda}^2 + \tilde{a}_1(c, \mu)\hat{\lambda} + \tilde{a}_0(c, \mu))\tilde{\mathcal{E}}(\hat{\lambda}, c; \mu) \\ &= \underbrace{[\tilde{a}_0(c, \mu)\tilde{e}_0(c, \mu)]}_{\stackrel{!}{=}a_0(c, \mu)} + \underbrace{[\tilde{a}_1(c, \mu)\tilde{e}_0(c, \mu) + \tilde{a}_0(c, \mu)\tilde{e}_1(c, \mu)]}_{\stackrel{!}{=}a_1(c, \mu)} \lambda \\ &\quad + \underbrace{[\tilde{e}_0(c, \mu) + \tilde{a}_1(c, \mu)\tilde{e}_1(c, \mu) + \tilde{a}_0(c, \mu)\tilde{e}_2(c, \mu)]}_{\stackrel{!}{=}a_2(c, \mu)} \lambda^2 + \dots \end{aligned}$$

At $(c, \mu) = (0, 0)$ we, hence, get

$$\begin{aligned} a_0(0, 0) &= \tilde{a}_0(0, 0)\tilde{e}_0(0, 0), \\ a_1(0, 0) &= \tilde{a}_1(0, 0)\tilde{e}_0(0, 0) + \tilde{a}_0(0, 0)\tilde{e}_1(0, 0), \\ a_2(0, 0) &= \tilde{e}_0(0, 0) + \tilde{a}_1(0, 0)\tilde{e}_1(0, 0) + \tilde{a}_0(0, 0)\tilde{e}_2(0, 0), \dots \end{aligned}$$

Since we know that $a_0(0, 0) = \frac{1}{4}\kappa_1^0|_{\mu=0} = 0$ and $\tilde{e}_0(0, 0) \neq 0$, we can conclude that $\tilde{a}_0(0, 0) = 0$, so $a_1(0, 0) = \tilde{a}_1(0, 0)\tilde{e}_0(0, 0)$. But since $a_1(0, 0) = -\frac{3}{16}\kappa_2^0|_{\mu=0} = 0$ and $\tilde{e}_0(0, 0) \neq 0$, this also implies $\tilde{a}_1(0, 0) = 0$. Hence, the above recursion simplifies to

$$a_{j+2}(0, 0) = \tilde{e}_j(0, 0), \quad j \geq 0. \tag{42}$$

In particular,

$$\tilde{e}_0(0, 0) = a_{02}(0), \quad \text{and} \quad \tilde{e}_1(0, 0) = a_{03}(0),$$

with a_{ij} from (34). Equipped with this information, we go to the second step and compare the leading order terms in the Taylor expansions (41) to infer the g_{j0} , that is, the coefficients at the SBT point. We immediately get

$$g_{10} = -\tilde{a}_0(0, 0) = 0, \quad \text{and} \quad g_{20} = -\tilde{a}_1(0, 0) = 0.$$

In order to compare the higher-order terms in the Taylor expansion, we have to take derivatives of the above recursion. This implies (where a similar reasoning as before gives $\partial_c \tilde{a}_0(0, 0) = 0$)

$$\begin{aligned} \partial_c^2 [\tilde{a}_0(c, \mu)\tilde{e}_0(0, 0)] \Big|_{(c, \mu)=(0, 0)} &= \partial_c^2 a_0(0, 0) \\ \Leftrightarrow \partial_c^2 \tilde{a}_0(0, 0) &= \frac{\partial_c^2 a_0(0, 0)}{\tilde{e}_0(0, 0)} = 2 \frac{a_{20}(0)}{a_{02}(0)}. \end{aligned}$$

The claimed expression for g_{30} now immediately follows from

$$3 \cdot 2 g_{30} = -\partial_c^2 \tilde{a}_0(0, 0).$$

A slightly longer, but analogous reasoning gives

$$\begin{aligned} \partial_c^2[\tilde{a}_1(c, \mu)\tilde{e}_0(c, \mu) + \tilde{a}_0(c, \mu)\tilde{e}_1(c, \mu)]|_{(c,\mu)=(0,0)} &= \partial_c^2 a_1(0, 0) \\ \Leftrightarrow \partial_c^2 \tilde{a}_1(c, \mu) &= \frac{1}{\tilde{e}_0(0, 0)} \left(\partial_c^2 a_1(0, 0) - (\partial_c^2 \tilde{a}_0(0, 0))\tilde{e}_1(0, 0) \right) \\ &= \frac{1}{\tilde{e}_0(0, 0)} \left(\partial_c^2 a_1(0, 0) - \frac{\partial_c^2 a_0(0, 0)}{\tilde{e}_0(0, 0)} \tilde{e}_1(0, 0) \right). \end{aligned}$$

So we infer the claimed g_{40} from

$$2 g_{40} = -\partial_c^2 \tilde{a}_1(0, 0) = -\frac{1}{a_{02}(0)} \left(2a_{21}(0) - 2\frac{a_{20}(0)}{a_{02}(0)} a_{03}(0) \right).$$

It remains to compute the expressions that yield the unfolding parameters. To this end, we need the linear terms in the Taylor expansion of \tilde{a}_0, \tilde{a}_1 with respect to μ , that is, we again have to differentiate, but this time with respect to μ . Using again $\tilde{a}_0(0, 0) = 0$ this gives

$$\nabla_\mu a_0(0, 0) = \nabla_\mu [\tilde{a}_0(c, \mu)\tilde{e}_0(c, \mu)]|_{(c,\mu)=(0,0)} \Leftrightarrow \nabla_\mu \tilde{a}_0(0, 0) = \frac{\nabla_\mu a_0(0, 0)}{\tilde{e}_0(0, 0)},$$

so that

$$g_{11} = -\nabla_\mu \tilde{a}_0(0, 0) = -\frac{\nabla_\mu a_0(0)}{a_{02}(0)},$$

and

$$\begin{aligned} \nabla_\mu a_1(0, 0) &= \nabla_\mu [\tilde{a}_1(c, \mu)\tilde{e}_0(c, \mu) + \tilde{a}_0(c, \mu)\tilde{e}_1(c, \mu)]|_{(c,\mu)=(0,0)} \\ \Leftrightarrow \nabla_\mu \tilde{a}_1(0, 0) &= \frac{1}{\tilde{e}_0(0, 0)} \left(\nabla_\mu a_1(0, 0) - \nabla_\mu \tilde{a}_0(0, 0)\tilde{e}_1(0, 0) \right) \\ &= \frac{1}{\tilde{e}_0(0, 0)} \left(\nabla_\mu a_1(0, 0) - \frac{\nabla_\mu a_0(0, 0)}{\tilde{e}_0(0, 0)} \tilde{e}_1(0, 0) \right). \end{aligned}$$

Now using (42), we get

$$g_{21} = -\frac{1}{a_{02}(0)} \left(\nabla_\mu a_{01}(0) - \frac{\nabla_\mu a_{00}(0)}{a_{02}(0)} a_{03}(0) \right).$$

Finally, the statement about g_{31}, g_{41} follows by continuity. This completes the proof of the lemma.

In order to verify the expressions in the corollary, we use the explicit expressions from (34). Noting that $\kappa_1^0 = \kappa_2^0 = 0$ implies

$$\alpha = \frac{2\sqrt{2}\hat{\theta}}{3\hat{\tau}(\hat{\theta} - \hat{\tau})}, \beta = \frac{2\sqrt{2}D\hat{\tau}}{3(\hat{\tau} - \hat{\theta})\hat{\theta}}, \tag{43}$$

we thus find

$$\tilde{e}_0(0, 0) = a_{02}|_{\kappa_1^0=0, \kappa_2^0=0} = -\frac{5\sqrt{2}}{48}\hat{\tau}\hat{\theta} < 0.$$

Furthermore,

$$g_{11} = \frac{48}{5\sqrt{2}\hat{\tau}\hat{\theta}}\nabla_{\mu}a_0\Big|_{\mu=0} = \frac{12}{5\sqrt{2}\hat{\tau}\hat{\theta}}\nabla_{\mu}\kappa_1^0\Big|_{\mu=0}$$

$$g_{21} = -\frac{48}{80\sqrt{2}\hat{\tau}\hat{\theta}}\left(3\nabla_{\mu}\kappa_2^0 - \frac{7}{2}(\hat{\tau} + \hat{\theta})\nabla_{\mu}\kappa_1^0\right)\Big|_{\mu=0},$$

where we used that $a_3|_{(c,\mu)=(0,0)} = -\frac{35}{256}\left(\alpha\hat{\tau}^4 + \frac{\beta}{D}\hat{\theta}^4\right)\Big|_{\mu=0}$ gives

$$\frac{a_3}{a_2}\Big|_{(c,\mu)=(0,0)} = -\frac{7}{8}(\hat{\tau} + \hat{\theta})\Big|_{\mu=0}.$$

Finally,

$$g_{30} = -\frac{3\sqrt{2}}{20}\left(\frac{\kappa_3^0}{\hat{\tau}\hat{\theta}}\right)\Big|_{\mu=0},$$

$$g_{40} = -\frac{3}{40}\frac{3(D^2\hat{\tau}^2 - \hat{\theta}^2) + 7\hat{\tau}\hat{\theta}(1 - D^2)}{D^2(\hat{\tau} - \hat{\theta})}\Big|_{\mu=0},$$

where the latter follows from simplifying, at $\kappa_1^0 = \kappa_2^0 = 0$, the expression

$$-\frac{1}{a_{02}(0)}\left(a_{21}(0) - \frac{a_{03}(0)}{a_{02}(0)}a_{20}(0)\right)$$

$$= \frac{24\sqrt{2}}{5\hat{\tau}\hat{\theta}}\left(\frac{15}{128}\left(\alpha\hat{\tau}^4 + \frac{\beta}{D^3}\hat{\theta}^4\right) + \frac{35}{256}\left(\alpha\hat{\tau}^4 + \frac{\beta}{D}\hat{\theta}^4\right)\frac{24\sqrt{2}}{5\hat{\tau}\hat{\theta}}\frac{3}{32}\kappa_3^0\right)\Big|_{\mu=0},$$

using that at $\mu = 0$ we have

$$\alpha\hat{\tau}^4 + \frac{\beta}{D^3}\hat{\theta}^4 = -\frac{2\sqrt{2}}{3}\hat{\tau}\hat{\theta}\frac{D^2\hat{\tau}^2 - \hat{\theta}^2}{D^2(\hat{\tau} - \hat{\theta})}, \quad \alpha\hat{\tau}^4 + \frac{\beta}{D}\hat{\theta}^4 = -\frac{2\sqrt{2}}{3}(\hat{\tau}\hat{\theta}(\hat{\tau} + \hat{\theta})).$$

The special case $g_{30} = 0$ means $D^2 = \frac{\hat{\tau}}{\hat{\theta}}$ and $\hat{\theta} \neq \hat{\tau}$, which imply $g_{40} = -\frac{3}{4}\hat{\tau} < 0$ based on these formulas. Moreover, if $\hat{\tau} = \frac{3}{7}\hat{\theta}$ then $g_{40} = -\frac{9}{28}\hat{\theta} \neq 0$, and $g_{40} = 0$ is equivalent to $\hat{\tau} \neq \hat{\theta}$ and $D^2 = \frac{\hat{\theta}}{\hat{\tau}}\frac{3\hat{\theta}-7\hat{\tau}}{3\hat{\tau}-7\hat{\theta}}$, which must be positive. The numerator is positive if $3\hat{\theta} > 7\hat{\tau}$, and the denominator is positive if $7\hat{\theta} < 3\hat{\tau}$. So, both must be negative, which holds for $\frac{3}{7} < \frac{\hat{\theta}}{\hat{\tau}} < \frac{7}{3}$. In this case, $g_{30} = \frac{2\hat{\tau}}{7\hat{\tau}-3\hat{\theta}} > 0$.

Concluding the proof, we show that $g_{30} < 0$ implies $g_{40} < 0$. For brevity, define $y := \frac{\hat{\theta}}{\hat{\tau}}$. Then, $g_{30} < 0$ is equivalent to $1 < y < D^2$ due to the standing assumption that $D > 1$. So, we assume that $1 < y < D^2$ and note that $g_{40} > 0$ is equivalent to $h(y) := \frac{7}{3}(D^2 - 1) - \frac{D^2}{y} + y < 0$. Since $h'(y) = \frac{D^2}{y^2} + 1 > 0$, the function h is strictly monotonically increasing and $h(1) = \frac{4}{3}(D^2 - 1) > 0$. In other words, $h(y) > 0$ for $1 < y < D^2$ and, thus, $g_{40} < 0$ if $g_{30} < 0$. \square

In the statement and proof of Proposition 3, we used (43) so that g_3, g_4 at $\mu = 0$ are independent of α, β . Then, it is natural to fix $\hat{\tau}, \hat{\theta}$ and choose μ affine in α, β as

$$\mu = (\alpha, \beta) - \frac{2\sqrt{2}}{3(\hat{\theta} - \hat{\tau})} \begin{pmatrix} \hat{\theta} \\ \hat{\tau} \end{pmatrix} - \frac{D\hat{\tau}}{\hat{\theta}}. \tag{44}$$

With this choice (37), (38) together with (6) give the matrix

$$\partial_{(\alpha, \beta)} \begin{pmatrix} g_1 \\ g_2 \end{pmatrix} \Big|_{\mu=0} = \frac{3\sqrt{2}}{5} \begin{pmatrix} \frac{2}{\hat{\theta}} & \frac{2}{D\hat{\tau}} \\ \frac{\hat{\tau}+7\hat{\theta}}{4\hat{\theta}} & \frac{\hat{\theta}+7\hat{\tau}}{4D\hat{\tau}} \end{pmatrix}. \tag{45}$$

We can now prove the main result concerning the unfolding of the SBT case, i.e., the triple zero eigenvalue of the PDE without additional degeneracy. The corresponding bifurcation diagram in the case $g_{30}, g_{40} < 0$ for the expansion (32) is as plotted in Fig. 3.

Theorem 2 *Let $\hat{\tau}, \hat{\theta} > 0, D > 1$ and $0 < \varepsilon \ll 1$. For $D^2\hat{\tau} \neq \hat{\theta}$ and $D^2\hat{\tau}(3\hat{\tau} - 7\hat{\theta}) \neq \hat{\theta}(3\hat{\theta} - 7\hat{\tau})$ the parameters α, β unfold the bifurcation point $\kappa_1^0 = \kappa_2^0 = 0$ of fronts in the sense of unfolding the SBT case for the reduced vector field (28) within the odd symmetry class of G .*

Proof Due to Proposition 3, $D^2\hat{\tau} \neq \hat{\theta}$ and $D^2\hat{\tau}(3\hat{\tau} - 7\hat{\theta}) \neq \hat{\theta}(3\hat{\theta} - 7\hat{\tau})$ imply $g_{30}, g_{40} \neq 0$, which are precisely the non-degeneracy conditions (H1), (H2) in Carr (1981, Chapter 4) for the vector field (28) with expansion (32); the condition (H3) in that reference holds since (28) is in second-order form.

The unfolding parameters in Carr (1981, Chapter 4) are $g_1 (= \partial_c G_1(0))$ and $g_2 (= G_2(0))$. The matrix (45) has determinant $\frac{54}{25} \frac{\hat{\tau} - \hat{\theta}}{D\hat{\tau}\hat{\theta}} \neq 0$ since $\hat{\tau} \neq \hat{\theta}$ if $\kappa_1^0 = \kappa_2^0 = 0$. It follows that near the SBT point $g_1 = g_2 = 0$, the mapping $(g_1, g_2) \mapsto (\alpha, \beta)$ is invertible. This and the signs of g_{30}, g_{40} persist for $0 < \varepsilon \ll 1$ by continuity. \square

Remark 3 Recall that due to Corollary 1, the case $g_{30} < 0$ and $g_{40} > 0$ cannot occur in (32). Otherwise, this would correspond to reflecting the case $g_{30} < 0$ and $g_{40} < 0$ by $(\tilde{c}, g_2, t) \rightarrow -(\tilde{c}, g_2, t)$. This means that the unfolding (with $\gamma = 0$) cannot generate stable ‘traveling breathers,’ i.e., periodically oscillating pseudo-fronts with nonzero average speed. In other words, there is no Hopf bifurcation from traveling fronts with $c \neq 0$ to stable periodic orbits in the reduced ODE.

Remark 4 Invoking the parameter γ breaks the odd symmetry of G as the existence condition for traveling fronts directly shows. Note that α, β will also unfold bifurcations for $|\gamma| > 0$ sufficiently small. In particular, consider the Hopf bifurcation for $g_{30}, g_{40}, g_1 < 0$ from stationary fronts to ‘standing breathers’ with zero average speed, labeled ho_1 in Fig. 3. Changing γ to a nonzero value will move this bifurcation point to a Hopf bifurcation that creates stable traveling breathers. We plot a numerical example in Fig. 7.

3.3 Numerical Continuation and Simulation

In this section, we present numerical computations that illustrate and corroborate the results of the previous sections. We use the software package `pde2path` (Uecker et al. 2014) for numerical continuation and bifurcation computations as well as simulations of the full PDE (1). Our focus lies on recovering numerically the theoretical bifurcations sketched in Fig. 3. As a starting point, we take the setting from Chirilus-Bruckner et al. (2015, Fig. 11), which shows a periodic solution found by direct numerical simulation near a triple root. We fix

$$\varepsilon = 0.03, \hat{\theta} = 10, \hat{\tau} = 4.21, D = 2.2 \quad (46)$$

and use a domain $[-L, L]$ with homogeneous Neumann boundary conditions. Unless noted otherwise we take $L = 10$, which turns out to be large enough so that longer domains do not noticeably change the results.

The numerical simulations of the time evolution for pseudo-fronts were done using the ‘freezing method’, cf. Beyn and Thümmler (2004) and Rademacher and Uecker (2017), where the domain moves effectively along with the traveling front in a comoving frame $\zeta(t) = x - a(t)$ with velocity $\frac{d}{dt}a = c$ of the pseudo-front (recall that in the analysis the velocity was rescaled to slow time). The instantaneous velocity is determined in each time step through the orthogonality condition to the group orbit of the translation symmetry given by

$$c(t) = \frac{\langle M^{-1}F(Z), Z_x \rangle}{\|Z_x\|_2^2}.$$

In the comoving ζ -coordinate, we can work on a relatively short spatial interval and with a fixed grid that is refined near the center, where the gradients are concentrated. We compute the ‘position’ based on this velocity as $a(t) = \int_0^t c(s) ds$, but note that in general dynamic pseudo-fronts move relative to the ζ variable. For instance, in bifurcating periodic solutions the zero intersection of the u -component is not stationary in ζ but moves periodically.

Recall that the theoretical values of the center manifold coefficients g_j from the previous sections were computed in the singular limit $\varepsilon = 0$. Since $\varepsilon > 0$ in the numerical computations, we expect the values differ slightly from the numerical ones, which we therefore denoted by \mathfrak{g}_j . We approximate \mathfrak{g}_3 and \mathfrak{g}_4 using the formulas from Corollary 1 and take α, β as affine functions of \mathfrak{g}_1 and \mathfrak{g}_2 through (44) and (45).

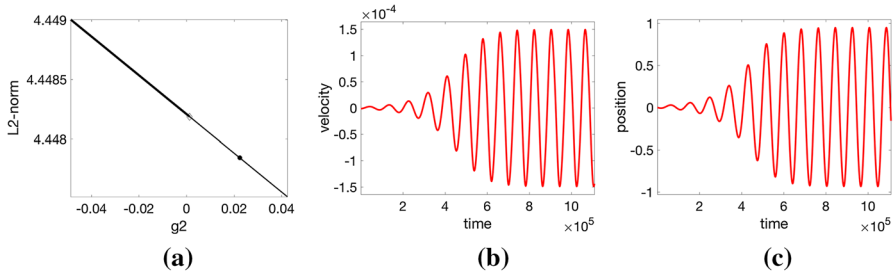


Fig. 4 From region 1 to 2 of Fig. 3, i.e., $g_3 \approx -0.074$, $g_4 \approx -3.14$ with $g_1 \approx -0.005$, and (46). **a** Branch of fronts from numerical continuation (stable thick, unstable thin) destabilizing at a Hopf bifurcation point (diamond) at $g_2 \approx 0.001$, theoretically predicted for $g_{30}, g_{40} < 0$ at $g_2 = 0$. **b, c** Plots of velocity and position from a simulation of a perturbation from the solution at the bullet in **a**, where $g_2 \approx 0.02$, and PDE parameters in (1) are $\alpha \approx 0.45$, $\beta \approx -0.24$ and (46)

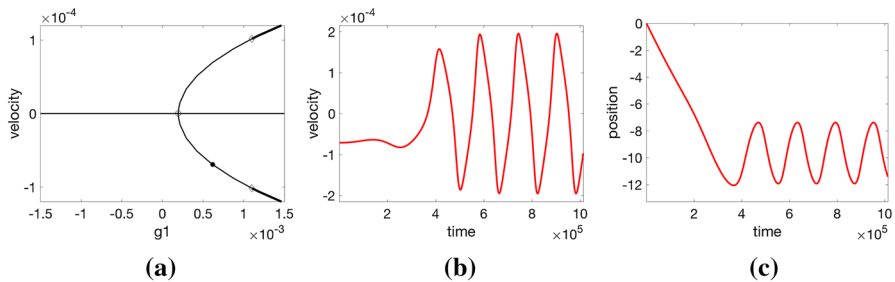


Fig. 5 From region 2 to 3,4 of Figure 3, i.e., $g_3 \approx -0.074$, $g_4 \approx -3.14$ with $g_2 = 0.042$, and (46). **a** Branches of fronts from numerical continuation (stable thick, unstable thin) connected at a pitchfork bifurcation at $g_1 \approx 0.0002$ stabilizing at Hopf points (diamonds) at $g_1 \approx 0.001$, matching the theoretical prediction. **b, c** Plots of velocity and position from a simulation of a perturbation from the solution at the bullet in **a**, where $g_1 \approx 0.0006$, and PDE parameters in (1) are $\alpha \approx 0.44$, $\beta \approx -0.19$ and (46). See also Fig. 2

The results plotted in Figs. 4 and 5 correspond to the crossing from region 1 of Fig. 3 to region 2 – a Hopf bifurcation—and further to regions 3 and 4 – a pitchfork bifurcation followed by another Hopf bifurcation. The crossing from region 1 to region 6 in Fig. 3, i.e., crossing the g_2 -axis with $g_2 < 0$, corresponds to the results plotted in Fig. 6. Here, a pitchfork bifurcation occurs, near which the emerging heteroclinic connection lies in a one-dimensional center manifold and is thus monotone. However, the phase portrait plotted for region 6 in Fig. 3 illustrates the case of complex leading eigenvalues of the bifurcated stable equilibrium. This highlights the underlying two-dimensional dynamics, which we find also numerically, as plotted in Fig. 6b.

Finally, as noted in Remark 4 for $\gamma = 0$ there are no stable periodic traveling fronts with nonzero average speed, while for $\gamma \neq 0$ these can be created. We plot an example in Fig. 7.

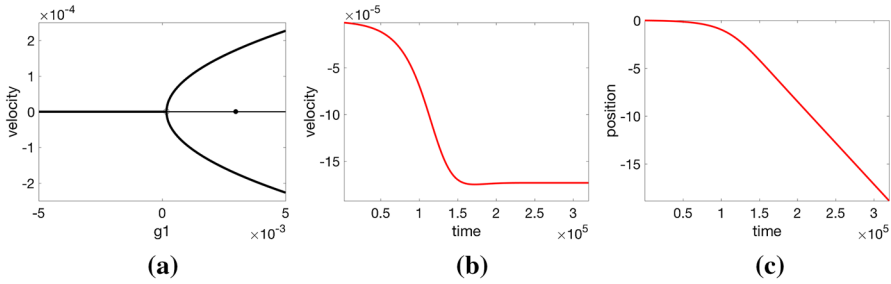


Fig. 6 From region 1 to 6 of Fig. 3, i.e., $g_3 \approx -0.074$, $g_4 \approx -3.14$ with $g_2 \approx -0.02$, and (46). **a** Branches of fronts from numerical continuation (stable thick, unstable thin) connected at a pitchfork bifurcation at $g_1 \approx 0.003$. **b, c** Plots of velocity and position from a simulation of a perturbation from the solution at the bullet in **a** with inset a magnification to highlight the oscillatory convergence. Here $g_1 \approx 0.003$, and PDE parameters in (1) are $\alpha \approx 0.34$, $\beta \approx -0.09$ and (46)

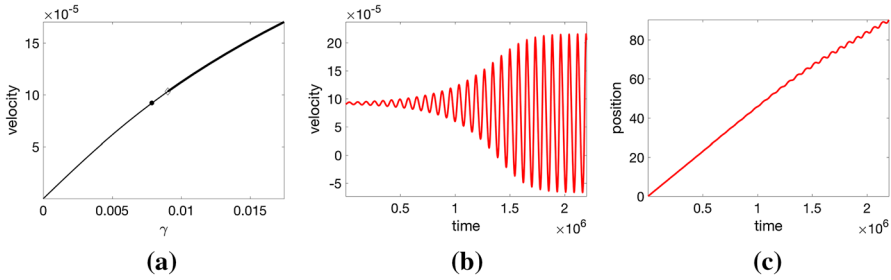


Fig. 7 Symmetry breaking with the parameter γ . **a** branch from numerical continuation starting at the rightmost point in Fig. 4a. **b, c** plots of velocity and position from a simulation upon perturbing at the point marked with a bullet in **a**, and PDE parameters in (1) are $\alpha \approx 0.48$, $\beta \approx -0.27$ and (46), See also Fig. 2

4 Conclusions and Outlook

We have demonstrated novel aspects in the rich dynamics of front solutions in the PDE (1) by focusing on instabilities of stationary front solutions. Specifically, we gave a rigorous analysis revealing that the temporal evolution of the velocity of fronts is governed by a planar ODE, and we unfolded the bifurcation scenario of a Bogdanov–Takens point with symmetry for these. The main novelties of the present work consist of the rigorous argument for the existence of a second generalized eigenfunction for the operator arising from linearization around a stationary front, and in the effective method to compute the critical coefficients for the reduced system on the center manifold using solely information on the previously computed Evans function and existence condition for uniformly traveling fronts.

These results put us in a position to analyze the unfolding of the triple zero eigenvalue for front dynamics in the PDE (1) with higher degeneracies: either the SBTB case or the imprint of a butterfly catastrophe in the SBTB case, see Definition 1. These higher codimension problems require determining an additional center manifold coefficient, and also pose challenges on the level of the unfolding theory for ODEs, e.g., Khibnik et al. (1998).

Equipped with the presented framework, we expect to find Jordan chains of higher order upon addition of more slow components. That is, for the $(n + 1)$ -component system with the perturbed Allen–Cahn ‘fast’ component U coupled to n ‘slow’ linear equations. In particular, such a 4-component system

$$\begin{cases} \partial_t U = \varepsilon^2 \partial_x^2 U + U - U^3 - \varepsilon \mathcal{G}(V_1, V_2, V_3), \\ \frac{\hat{\tau}_j}{\varepsilon^2} \partial_t V_j = D_j^2 \partial_x^2 V_j + U - V_j, \quad j = 1, 2, 3, \end{cases}$$

would yield a Jordan block of length four and, hence, a three-dimensional reduced system on the center manifold (after factoring out translations). By appropriately changing the coupling of all components to imprint the desired singularity structure, a similar analysis as illustrated here could lead to a normal form of a chaotic system, and thus to one of the rare cases where chaos can be rigorously proved in the context of a nonlinear PDE.

Acknowledgements PvH thanks Leiden University for its hospitality. JR notes this paper is a contribution to project M2 of the Collaborative Research Centre TRR 181 ‘Energy Transfer in Atmosphere and Ocean’ funded by the Deutsche Forschungsgemeinschaft (DFG, German Research Foundation)—Project Number 274762653. The authors also acknowledge that a crucial part of this paper was established during the first and second joint Australia–Japan workshop on dynamical systems with applications in life sciences.

A Leading Order Form of Eigenfunctions

In the proof of Proposition 2 and Remark 1, we use leading order information on the eigenfunction and first generalized eigenfunction for the zero eigenvalue. The corresponding statements and proofs can be found here in Lemmas 5 and 6. The section is completed by giving the leading order expressions for the second generalized eigenfunction in Lemma 7.

Lemma 5 (Leading order of the eigenfunctions) *The eigenfunctions $\Phi_{\hat{\lambda}}$ belonging to the small eigenvalues from Proposition 1 are to leading order given by*

$$\begin{bmatrix} 0 \\ h_v(\hat{\lambda})e^{h_v(\hat{\lambda})x} \\ h_w(\hat{\lambda})e^{h_w(\hat{\lambda})x} \end{bmatrix} \chi_{s-}(x) + \begin{bmatrix} \frac{1}{\varepsilon} \operatorname{sech}^2 \left[\frac{x}{\sqrt{2\varepsilon}} \right] \\ h_v(\hat{\lambda}) \\ h_w(\hat{\lambda}) \end{bmatrix} \chi_f(x) + \begin{bmatrix} 0 \\ h_v(\hat{\lambda})e^{-h_v(\hat{\lambda})x} \\ h_w(\hat{\lambda})e^{-h_w(\hat{\lambda})x} \end{bmatrix} \chi_{s+}(x),$$

with

$$h_v(\hat{\lambda}) = \frac{1}{\sqrt{\hat{\tau}\hat{\lambda} + 1}}, \quad h_w(\hat{\lambda}) = \frac{1}{D\sqrt{\hat{\theta}\hat{\lambda} + 1}}.$$

Proof Using the notation $\Phi_{\hat{\lambda}} = (u, v, w)$ for the eigenfunction corresponding to the eigenvalue $\lambda = \varepsilon^2 \hat{\lambda}$, the ODE arising from the eigenvalue problem (9) for small eigenvalues reads

$$\begin{cases} \varepsilon u' = p, \\ \varepsilon p' = \varepsilon^2 \hat{\lambda} u + (3(u^h)^2 - 1)u + \varepsilon(\alpha v + \beta w), \\ v' = q, \\ q' = (\hat{\tau} \hat{\lambda} + 1)v - u, \\ w' = r, \\ r' = \frac{1}{D^2}(\hat{\theta} \hat{\lambda} + 1)w - \frac{1}{D^2}u, \end{cases}$$

In the language of slow–fast ODEs, this is the slow system with corresponding fast system given by

$$\begin{cases} \dot{u} = p, \\ \dot{p} = \varepsilon^2 \hat{\lambda} u + (3(u^h)^2 - 1)u + \varepsilon(\alpha v + \beta w), \\ \dot{v} = \varepsilon q, \\ \dot{q} = \varepsilon(\hat{\tau} \hat{\lambda} + 1)v - \varepsilon u, \\ \dot{w} = \varepsilon r, \\ \dot{r} = \frac{\varepsilon}{D^2}(\hat{\theta} \hat{\lambda} + 1)w - \frac{\varepsilon}{D^2}u, \end{cases}$$

where the dot denotes differentiation with respect to $\xi = x/\varepsilon$. In the regions $I_{s\pm}$, we will use a regular expansion of the eigenfunction in the slow system, while in the regions I_f we will use a regular expansion of the eigenfunction in the fast system. In the following, we will use the following notation: Regular expansions of the amplitude will be denoted by $u = u_0 + \varepsilon u_1 + \varepsilon^2 u_2 + \dots$ and similarly for v, w and u^h . Furthermore, we add to the index ‘ f ’ in the fast field and ‘ $s\pm$ ’ in the slow fields.

Before we demonstrate the calculations, we would like to remark that we make use of the following observations from Chirilus-Bruckner et al. (2015) [which can already be found in Doelman et al. (2009)]: We have that

$$u_f^h = u_{0,f}^h + \varepsilon^2 u_{2,f}^h + \mathcal{O}(\varepsilon^3), \tag{47}$$

that is, there is no first-order correction of the stationary front in the fast field. Furthermore, we will need to use the value of the integral

$$6 \int_{-\infty}^{\infty} u_{0,f}^h(\xi) u_{2,f}^h(\xi) \operatorname{sech}^4 \left(\frac{1}{2} \sqrt{2} \xi \right) d\xi = -4 \left(\alpha + \frac{\beta}{D} \right). \tag{48}$$

Equipped with these facts, we will now recursively solve the perturbation hierarchy to construct an eigenfunction, i.e., a homoclinic to zero.

Fast field, $\mathcal{O}(1)$: We get for the u -component

$$\ddot{u}_{0,f} = \left(3(u_{0,f}^h)^2 - 1 \right) u_{0,f}, \quad u_{0,f}(\xi) = C \operatorname{sech} \left(\frac{1}{2} \sqrt{2} \xi \right), \quad C \in \mathbb{R}.$$

while $\dot{v}_{0,f} = \dot{q}_{0,f} = \dot{w}_{0,f} = \dot{r}_{0,f} = 0$. In order to compute the constant values assumed by these latter components, we need to switch to the slow fields.

Slow fields, $\mathcal{O}(1)$: We have $u_{0,s\pm} = p_{0,s\pm} = 0$, while the equations for v, w -components read

$$v''_{0,s\pm} = (\hat{\tau}\hat{\lambda} + 1)v_{0,s\pm}, \quad w''_{0,s\pm} = \frac{1}{D^2}(\hat{\theta}\hat{\lambda} + 1)w_{0,s\pm},$$

which are solved by exponentials. Using the information from the fast field that v, q, w, r are constant and matching slow and fast solutions gives that $v_{0,s\pm} = q_{0,s\pm} = w_{0,s\pm} = r_{0,s\pm} = 0$, therefore also $v_{0,f} = q_{0,f} = w_{0,f} = r_{0,f} = 0$.

Fast field, $\mathcal{O}(\varepsilon)$: We get for the u -component due to (47) and $v_{0,f} = w_{0,f} = 0$ again

$$\ddot{u}_{1,f} = \left(3(u_{0,f}^h)^2 - 1\right)u_{1,f}, \quad u_{1,f}(\xi) = \tilde{c}, \operatorname{sech}\left(\frac{1}{2}\sqrt{2}\xi\right), \quad \tilde{c} \in \mathbb{R}.$$

and we choose in this case $\tilde{c} = 0$ since, otherwise, this would simply add an ε correction to C from the leading order. Furthermore, we have $\dot{v}_{1,f} = \dot{w}_{1,f} = 0$ and

$$\dot{q}_{1,f} = -u_{0,f}, \quad \dot{r}_{1,f} = -\frac{1}{D^2}u_{0,f}. \tag{49}$$

Again, in order to compute the constant values assumed by these latter components we need to switch to the slow fields.

Slow fields, $\mathcal{O}(\varepsilon)$: We have $u_{1,s\pm} = p_{1,s\pm} = 0$, while the equations for v, w -components read

$$v''_{1,s\pm} = (\hat{\tau}\hat{\lambda} + 1)v_{1,s\pm}, \quad w''_{1,s\pm} = \frac{1}{D^2}(\hat{\theta}\hat{\lambda} + 1)w_{1,s\pm},$$

which is solved by

$$v_{1,s\pm}(x) = A_{\pm}e^{\mp\sqrt{\hat{\tau}\hat{\lambda}+1}x}, \quad w_{1,s\pm}(x) = B_{\pm}e^{\mp\frac{1}{D}\sqrt{\hat{\theta}\hat{\lambda}+1}x},$$

where we already took into account that the eigenfunction components need to approach zero at the infinities. Again matching these solutions over the fast fields using $v_{1,s-}(0) = v_{1,s+}(0), w_{1,s-}(0) = w_{1,s+}(0)$ gives $A_+ = A_- =: A, B_+ = B_- =: B$. Furthermore, matching the q, r -components using (49) gives

$$\begin{aligned} q_{1,s+}(0) - q_{1,s-}(0) &= \int_{-\infty}^{\infty} \dot{q}_{1,f}(\xi) d\xi = \\ &= -\int_{-\infty}^{\infty} u_{0,f}(\xi) d\xi = -2\sqrt{2}C = -2A\sqrt{\hat{\tau}\hat{\lambda} + 1}, \end{aligned}$$

hence, $A = \sqrt{2}C/\sqrt{\hat{\tau}\hat{\lambda} + 1}$. The analogous procedure for the r -component gives $B = \sqrt{2}C/(D\sqrt{\hat{\theta}\hat{\lambda} + 1})$. Hence, the values of the components in the fast fields are $v_{1,f} = A, w_{1,f} = B$.

Fast field, $\mathcal{O}(\varepsilon^2)$: We get for the u -component due to (47) the equation

$$\ddot{u}_{2,f} = \left(3(u_{0,f}^h)^2 - 1\right)u_{2,f} + 6u_{0,f}^h u_{2,f}^h u_{0,f} + \alpha v_{1,f} + \beta w_{1,f} + \hat{\lambda}u_{0,f},$$

for which we enforce the solvability condition

$$\underbrace{6 \int_{-\infty}^{\infty} u_{0,f}^h(\xi) u_{2,f}^h(\xi) u_{0,f}^2(\xi) d\xi}_{=-4C^2(\alpha+\beta/D)} + \left(\alpha \frac{\sqrt{2}C}{\sqrt{\hat{\tau}\hat{\lambda} + 1}} + \beta \frac{\sqrt{2}C}{D\sqrt{\hat{\theta}\hat{\lambda} + 1}} \right) \underbrace{\int_{-\infty}^{\infty} u_{0,f}(\xi) d\xi}_{=2\sqrt{2}C} + \hat{\lambda} \underbrace{\int_{-\infty}^{\infty} u_{0,f}(\xi)^2 d\xi}_{=C^2(4\sqrt{2}/3)} = 0,$$

where we made use of (48). Note that C drops out of the equation since, of course, eigenfunctions are only unique up to multiplication with a constant. We choose in the statement of the proposition $C = \frac{1}{2}\sqrt{2}/\varepsilon$, since this scaling naturally arises when computing the eigenfunction for $\lambda = 0$ through differentiation of the stationary front. □

Lemma 6 (Leading order of first generalized eigenfunction) *Let the parameters be chosen such that (7) is satisfied, that is, that the zero eigenvalue has algebraic multiplicity two. Then, there is a generalized eigenfunction Ψ which is to leading order given by*

$$\begin{bmatrix} \Psi_u(x) \\ \Psi_v(x) \\ \Psi_w(x) \end{bmatrix} = \begin{bmatrix} \varepsilon u_{s-}(x) \\ v_{0,s-}(x) \\ w_{0,s-}(x) \end{bmatrix} \chi_{s-}(x) + \begin{bmatrix} \frac{\varepsilon}{3\sqrt{2}} \\ -\frac{\hat{\tau}}{2} \\ -\frac{\hat{\theta}}{2D} \end{bmatrix} \chi_f(x) + \begin{bmatrix} \varepsilon u_{s+}(x) \\ v_{0,s+}(x) \\ w_{0,s+}(x) \end{bmatrix} \chi_{s+}(x), \tag{50}$$

with

$$v_{0,s\pm}(x) = -\frac{1}{2}\hat{\tau}(1 \pm x)e^{\mp x}, \quad w_{0,s\pm}(x) = -\frac{1}{2}\frac{\hat{\theta}}{D} \left(1 \pm \frac{1}{D}x\right) e^{\mp x/D}.$$

and

$$u_{s,\pm}(x) = -\frac{1}{2}\alpha v_{0,s\pm}(x) - \frac{1}{2}\beta w_{0,s\pm}(x).$$

Proof For notational simplicity, we write $(\Psi_u, \Psi_v, \Psi_w) = (u, v, w)$. The ODE arising from the equation for the generalized eigenfunction reads

$$\begin{cases} \varepsilon u' = p, \\ \varepsilon p' = \varepsilon^2 \Phi_u + (3(u^h)^2 - 1)u + \varepsilon(\alpha v + \beta w), \\ v' = q, \\ q' = v + \hat{\tau} \Phi_v - u, \\ w' = r, \\ r' = \frac{1}{D^2} w + \frac{\hat{\theta}}{D^2} \Phi_w - \frac{1}{D^2} u, \end{cases}$$

recalling that Φ is the eigenfunction for the zero eigenvalue and u^h is the u -component of the front solution (3). The corresponding fast system given by

$$\begin{cases} \dot{u} = p, \\ \dot{p} = \varepsilon^2 \Phi_u + (3(u^h)^2 - 1)u + \varepsilon(\alpha v + \beta w), \\ \dot{v} = \varepsilon q, \\ \dot{q} = \varepsilon v + \varepsilon \hat{\tau} \Phi_v - \varepsilon u, \\ \dot{w} = \varepsilon r, \\ \dot{r} = \frac{\varepsilon}{D^2} w + \frac{\varepsilon}{D^2} \hat{\theta} \Phi_w - \frac{\varepsilon}{D^2} u, \end{cases}$$

where again the dot denotes differentiation with respect to $\xi = x/\varepsilon$.

Fast field, $\mathcal{O}(1)$: As before, we get

$$\ddot{u}_{0,f} = \left(3(u_{0,f}^h)^2 - 1\right)u_{0,f}, \quad \dot{v}_{0,f} = \dot{q}_{0,f} = \dot{w}_{0,f} = \dot{r}_{0,f} = 0,$$

We can choose $u_{0,f} = 0$ this time: On the one hand, its value will not change the computations later on (it will appear as product with $u_{1,f}^h$ which is zero), and on the other hand, it is already part of the eigenfunction itself. In order to compute the constant values assumed by the other components, we need to switch to the slow fields.

Slow fields, $\mathcal{O}(1)$: We have $u_{0,s\pm} = p_{0,s\pm} = 0$, while the equations for v, w -components read

$$v''_{0,s\pm} = v_{0,s\pm} + \hat{\tau} e^{\mp x}, \quad w''_{0,s\pm} = \frac{1}{D^2} w_{0,s\pm} + \frac{\hat{\theta}}{D^3} e^{\mp x/D}.$$

We have that

$$\begin{aligned} v_{0,s\pm}(x) &= A_{\pm} e^{\mp x} \mp \frac{1}{2} \hat{\tau} x e^{\mp x}, \\ w_{0,s\pm}(x) &= B_{\pm} e^{\mp x/D} \mp \frac{1}{2} \frac{\hat{\theta}}{D^2} x e^{\mp x/D}, \quad A_{\pm}, B_{\pm} \in \mathbb{R}. \end{aligned}$$

Matching with the information of the fast components $v_{1,s-}(0) = v_{1,s+}(0)$, $w_{1,s-}(0) = w_{1,s+}(0)$ gives $A_+ = A_- =: A$, $B_+ = B_- =: B$, while

$q_{1,s-}(0) = q_{1,s+}(0), r_{1,s-}(0) = r_{1,s+}(0)$ gives $A = -\hat{\tau}/2, B = -\hat{\theta}/(2D)$, so

$$v_{0,s\pm}(x) = -\frac{1}{2}\hat{\tau}(1 \pm x)e^{\mp x}, \quad w_{0,s\pm}(x) = -\frac{1}{2}\frac{\hat{\theta}}{D}\left(1 \pm \frac{1}{D}x\right)e^{\mp x/D}.$$

Hence, the values of the components in the fast fields are

$$v_{0,f} = -\frac{1}{2}\hat{\tau}, \quad w_{0,f} = -\frac{1}{2}\frac{\hat{\theta}}{D}.$$

Fast field, $\mathcal{O}(\varepsilon)$: We get for the u -component due to (47) and the fact that

$$\Phi_u(\xi) = \left(\frac{1}{\varepsilon}\right)\frac{1}{2}\sqrt{2}\operatorname{sech}^2\left(\frac{1}{2}\sqrt{2}\xi\right)$$

the equation

$$\ddot{u}_{1,f} = \left(3(u_{0,f}^h)^2 - 1\right)u_{1,f} + \frac{1}{2}\sqrt{2}\operatorname{sech}^2\left(\frac{1}{2}\sqrt{2}\xi\right)\underbrace{+\alpha v_{0,f} + \beta w_{0,f}}_{=-\left(\frac{1}{2}\alpha\hat{\tau} + \frac{1}{2}\frac{\beta}{D}\hat{\theta}\right)}$$

for which we get the solvability condition

$$\underbrace{\frac{1}{2}\sqrt{2}\int_{-\infty}^{\infty}\operatorname{sech}^4\left(\frac{1}{2}\sqrt{2}\xi\right)d\xi}_{=4/3} - \left(\frac{1}{2}\alpha\hat{\tau} + \frac{1}{2}\frac{\beta}{D}\hat{\theta}\right)\underbrace{\int_{-\infty}^{\infty}\operatorname{sech}^2\left(\frac{1}{2}\sqrt{2}\xi\right)d\xi}_{=2\sqrt{2}} = 0,$$

and, hence, the condition (7) which can also be written as $\mathcal{D}'(0) = 0$. Rewriting this condition as

$$-\left(\frac{1}{2}\alpha\hat{\tau} + \frac{1}{2}\frac{\beta}{D}\hat{\theta}\right) = -\frac{\sqrt{2}}{3},$$

and using the ansatz $u_{1,f} = K \in \mathbb{R}$, we get

$$0 = \left[3 \tanh^2\left(\frac{1}{2}\sqrt{2}\xi\right) - 1\right]K + \frac{1}{2}\sqrt{2}\operatorname{sech}^2\left(\frac{1}{2}\sqrt{2}\xi\right) - \frac{\sqrt{2}}{3},$$

which, by the identity $\operatorname{sech}^2(z) = 1 - \tanh^2(z)$ becomes

$$0 = \left[3 \tanh^2\left(\frac{1}{2}\sqrt{2}\xi\right) - 1\right]K + \frac{\sqrt{2}}{6}\left[1 - 3 \tanh^2\left(\frac{1}{2}\sqrt{2}\xi\right)\right],$$

which gives $K = \frac{1}{3\sqrt{2}}$. □

The previous lemma was used in the proof of Proposition 2 for the existence of a second generalized eigenfunction. Here, we give the formal computations that lead to first-order expressions for it.

Lemma 7 (Leading order of second generalized eigenfunction) *Let the parameters be chosen such that (8) is satisfied, that is, that the zero eigenvalue has algebraic multiplicity three. Then, there are two generalized eigenfunctions: Ψ as in Proposition 6 and $\tilde{\Psi}$ which is to leading order given by*

$$\begin{bmatrix} \tilde{\Psi}_u(x) \\ \tilde{\Psi}_v(x) \\ \tilde{\Psi}_w(x) \end{bmatrix} = \begin{bmatrix} \varepsilon \tilde{u}_{s-}(x) \\ \tilde{v}_{0,s-}(x) \\ \tilde{w}_{0,s-}(x) \end{bmatrix} \chi_{s-}(x) + \begin{bmatrix} \mathcal{O}(\varepsilon^2) \\ \frac{3\hat{\tau}^2}{8} \\ \frac{3\hat{\theta}^2}{8D} \end{bmatrix} \chi_f(x) + \begin{bmatrix} \varepsilon \tilde{u}_{s+}(x) \\ \tilde{v}_{0,s+}(x) \\ \tilde{w}_{0,s+}(x) \end{bmatrix} \chi_{s+}(x) + h.o.t..$$

with

$$\tilde{v}_{0,s\pm}(x) = \frac{1}{8} \hat{\tau}^2 (x^2 \pm 3x + 3) e^{\mp x}, \quad \tilde{w}_{0,s\pm}(x) = \frac{\hat{\theta}^2}{8D^3} (x^2 \pm 3Dx + 3D^2) e^{\mp x/D}.$$

and

$$\tilde{u}_{s,\pm}(x) = -\frac{1}{2} \alpha \tilde{v}_{0,s\pm}(x) - \frac{1}{2} \beta \tilde{w}_{0,s\pm}(x).$$

Proof For notational simplicity, we write $(\tilde{\Psi}_u, \tilde{\Psi}_v, \tilde{\Psi}_w) = (u, v, w)$. The ODE arising from the equation for the second generalized eigenfunction reads

$$\begin{cases} \varepsilon u' = p, \\ \varepsilon p' = \varepsilon^2 \Psi_u + (3(u^h)^2 - 1)u + \varepsilon(\alpha v + \beta w), \\ v' = q, \\ q' = v + \hat{\tau} \Psi_v - u, \\ w' = r, \\ r' = \frac{1}{D^2} w + \frac{\hat{\theta}}{D^2} \Psi_w - \frac{1}{D^2} u, \end{cases}$$

recalling that Ψ is the first generalized eigenfunction for the zero eigenvalue (50) and u^h is the u -component of the front solution (3). The corresponding fast system given by

$$\begin{cases} \dot{u} = p, \\ \dot{p} = \varepsilon^2 \Psi_u + (3(u^h)^2 - 1)u + \varepsilon(\alpha v + \beta w), \\ \dot{v} = \varepsilon q, \\ \dot{q} = \varepsilon v + \varepsilon \hat{\tau} \Psi_v - \varepsilon u, \\ \dot{w} = \varepsilon r, \\ \dot{r} = \frac{\varepsilon}{D^2} w + \frac{\varepsilon}{D^2} \hat{\theta} \Psi_w - \frac{\varepsilon}{D^2} u, \end{cases}$$

where again the dot denotes differentiation with respect to $\xi = x/\varepsilon$.

Fast field, $\mathcal{O}(1)$: Exactly as before, we get

$$\tilde{u}_{0,f} = \left(3(u_{0,f}^h)^2 - 1\right)\tilde{u}_{0,f}, \quad \tilde{v}_{0,f} = \tilde{q}_{0,f} = \tilde{w}_{0,f} = \tilde{r}_{0,f} = 0,$$

and once again we can choose $\tilde{u}_{0,f} = 0$, and switch to the slow fields to determine the constant values the remaining components assume.

Slow fields, $\mathcal{O}(1)$: We have $\tilde{u}_{0,s\pm} = p_{0,s\pm} = 0$, while the equations for v, w -components read

$$\begin{aligned} \tilde{v}_{0,s\pm}'' - \tilde{v}_{0,s\pm} &= -\frac{1}{2}\hat{\tau}^2(1 \pm x)e^{\mp x}, \\ D^2\tilde{w}_{0,s\pm}'' - \frac{1}{D^2}\tilde{w}_{0,s\pm} &= -\frac{1}{2}\frac{\hat{\theta}^2}{D}\left(1 \pm \frac{1}{D}x\right)e^{\mp x/D}. \end{aligned} \tag{51}$$

We have that

$$\begin{aligned} \tilde{v}_{0,s\pm}(x) &= Ae^{\mp x} + \frac{1}{8}\hat{\tau}^2(x^2 \pm 3x)e^{\mp x}, \\ \tilde{w}_{0,s\pm}(x) &= Be^{\mp x/D} + \frac{\hat{\theta}^2}{8D^3}(x^2 \pm 3Dx)e^{\mp x/D}, \end{aligned}$$

with $A, B \in \mathbb{R}$ and where we already used the matching with the information of the fast components

$$\tilde{v}_{1,s-}(0) = \tilde{v}_{1,s+}(0), \quad \tilde{w}_{1,s-}(0) = \tilde{w}_{1,s+}(0).$$

Furthermore, $q_{1,s-}(0) = q_{1,s+}(0), r_{1,s-}(0) = r_{1,s+}(0)$ gives

$$\tilde{v}_{0,s\pm}(x) = \frac{1}{8}\hat{\tau}^2(x^2 \pm 3x + 3)e^{\mp x}, \quad \tilde{w}_{0,s\pm}(x) = \frac{\hat{\theta}^2}{8D^3}(x^2 \pm 3Dx + 3D^2)e^{\mp x/D}.$$

Hence, the values of the components in the fast fields are

$$\tilde{v}_{0,f} = \frac{3}{8}\hat{\tau}^2, \quad \tilde{w}_{0,f} = \frac{3}{8}\frac{\hat{\theta}^2}{D}. \tag{52}$$

Fast field, $\mathcal{O}(\varepsilon)$: We get for the u -component due to (47) the equation

$$\check{u}_{1,f} = \left(3(u_{0,f}^h)^2 - 1\right)\tilde{u}_{1,f} + \alpha\tilde{v}_{0,f} + \beta\tilde{w}_{0,f},$$

for which we get the solvability condition

$$\frac{3}{8}\left(\alpha\hat{\tau}^2 + \frac{\beta}{D}\hat{\theta}^2\right)\underbrace{\int_{-\infty}^{\infty} \operatorname{sech}^2\left(\frac{1}{2}\sqrt{2}\xi\right)d\xi}_{=2\sqrt{2}} = 0,$$

and, hence, the triple zero eigenvalue condition (8), which can also be written as $\mathcal{D}''(0) = 0$. Since by this condition, we again recover

$$\tilde{u}_{1,f} = \left(3(u_{0,f}^h)^2 - 1\right)\tilde{u}_{1,f},$$

we choose with a similar argument as before $\tilde{u}_{1,f} = 0$. □

B Proof of Lemma 1 (Spectrum of the Operator L_ε)

Introducing the notation

$$\Phi = \begin{pmatrix} \Phi_u \\ \Phi_{v,w} \end{pmatrix},$$

for the eigenfunction of the zero eigenvalue, we can write the corresponding eigenvalue problem as

$$\begin{pmatrix} L_\varepsilon & \varepsilon A \\ B & S \end{pmatrix} \begin{pmatrix} \Phi_u \\ \Phi_{v,w} \end{pmatrix} = \begin{pmatrix} 0 \\ 0 \end{pmatrix}.$$

By solving the second equation for $\Phi_{v,w}$, we get $\Phi_{v,w} = -S^{-1}B\Phi_u$, and inserted into the first equation this gives

$$L_\varepsilon\Phi_u = \varepsilon AS^{-1}B\Phi_u.$$

Recalling that L_ε has the form

$$L_\varepsilon = \varepsilon^2\partial_x^2 + \left(1 - 3u_0^h\left(\frac{x}{\varepsilon}\right)^2\right) + \mathcal{O}(\varepsilon^2),$$

we change to the fast variable to $y = \frac{x}{\varepsilon}$ and write

$$L_\varepsilon = L_0 + \varepsilon^2L_1 + \dots,$$

with

$$L_0 = \partial_y^2 + \left(1 - 3u_0^h(y)^2\right).$$

Note that since S^{-1} is a convolution operator with respect to x , changing to $y = \frac{x}{\varepsilon}$ gives an additional factor of ε , so we write $S^{-1} = \varepsilon\bar{S}^{-1}$, where now \bar{S}^{-1} gives the convolution with respect to y . Furthermore, we set

$$\Phi_u(y) = \frac{1}{\varepsilon}\phi_0(y) + \varepsilon\phi_1(y) + \dots,$$

and after plugging all these expanded quantities back into

$$L_\varepsilon \Phi_u = \varepsilon^2 A \bar{S}^{-1} B \Phi_u,$$

we get the equation for Φ_1 given by

$$L_0 \Phi_1 = -L_1 \phi_0 + A \bar{S}^{-1} B \phi_0,$$

which yields the solvability condition

$$\langle L_1 \phi_0, \phi_0 \rangle = \langle A \bar{S}^{-1} B \phi_0, \phi_0 \rangle. \quad (53)$$

Equipped with this, we can now turn to the eigenvalue problem

$$L_\varepsilon \phi = \varepsilon^2 \tilde{\mu}_\varepsilon \phi.$$

Setting $\phi = \frac{1}{\varepsilon} \phi_0 + \varepsilon \phi_1 + \dots$, $\tilde{\mu}_\varepsilon = \tilde{\mu}_0 + \dots$ (noting that Φ_u and ϕ must coincide in leading order, but might differ in the next orders), we get

$$L_0 \phi_1 = -L_1 \phi_0 + \tilde{\mu}_0 \phi_0,$$

yielding the solvability condition

$$\tilde{\mu}_0 = \frac{\langle L_1 \phi_0, \phi_0 \rangle}{\langle \phi_0, \phi_0 \rangle}. \quad (54)$$

Combining (53) and (54) gives

$$\tilde{\mu}_0 = \frac{\langle A \bar{S}^{-1} B \phi_0, \phi_0 \rangle}{\langle \phi_0, \phi_0 \rangle}.$$

Finally, using that $\bar{S}^{-1} = \frac{1}{\varepsilon} S^{-1}$ and that $\frac{1}{\varepsilon} \phi_0 \left(\frac{x}{\varepsilon} \right)$ is a Dirac sequence, we get as claimed in the limit $\varepsilon \rightarrow 0$

$$\tilde{\mu}_0 = \frac{3\sqrt{2}}{2} \left(\alpha + \frac{\beta}{D} \right).$$

References

- Alexander, J.C., Gardner, R.A., Jones, C.K.R.T.: A topological invariant arising in the stability analysis of traveling waves. *J. Reine Angew. Math.* **410**, 167–212 (1990)
- Bellsky, T., Doelman, A., Kaper, T.J., Promislow, K.: Adiabatic stability under semi-strong interactions: the weakly damped regime. *Indiana U. Math. J.* **62**, 1809–1859 (2014)
- Bejn, W.-J., Thümmel, V.: Freezing solutions of equivariant evolution equations. *SIAM J. Appl. Dyn. Sys.* **3**, 85–115 (2004)

- Carr, J.: Applications of Centre Manifold Theory, vol. 35. Springer, Berlin (1981)
- Chow, S.-N., Hale, J.K.: Methods of Bifurcation Theory, vol. 62. Springer, Berlin (1982)
- Chen, C.-N., Choi, Y.S.: Standing pulse solutions to FitzHugh–Nagumo equations. Arch. Ration. Mech. Anal. **206**, 741–777 (2012)
- Chirilus-Bruckner, M., Doelman, A., van Heijster, P., Rademacher, J.D.M.: Butterfly catastrophe for fronts in a three-component reaction–diffusion system. J. Nonlinear Sci. **25**, 87–129 (2015)
- Doelman, A., Gardner, R.A., Kaper, T.J.: Large stable pulse solutions in reaction–diffusion equations. Indiana U. Math. J. **50**, 443–507 (2001)
- Doelman, A., Kaper, T.J.: Semistrong pulse interactions in a class of coupled reaction–diffusion equations. SIAM J. Appl. Dyn. Sys. **2**, 53–96 (2003)
- Doelman, A., Kaper, T.J., Promislow, K.: Nonlinear asymptotic stability of the semistrong pulse dynamics in a regularized Gierer–Meinhardt model. SIAM J. Math. Anal. **38**, 1760–1787 (2007)
- Doelman, A., van Heijster, P., Kaper, T.J.: Pulse dynamics in a three-component system: existence analysis. J. Dyn. Differ. Equ. **21**, 73–115 (2009)
- Ei, S.-I., Mimura, M., Nagayama, M.: Pulse-pulse interaction in reaction–diffusion systems. Phys. D **165**, 176–198 (2002)
- Hagberg, A., Meron, E.: Pattern formation in non-gradient reaction–diffusion systems: the effects of front bifurcations. Nonlinearity **7**, 805–835 (1994)
- Haragus, M., Iooss, G.: Local Bifurcations, Center Manifolds, and Normal Forms in Infinite-Dimensional Dynamical Systems. Springer, London (2011)
- Ikeda, H., Ikeda, T.: Bifurcation phenomena from standing pulse solutions in some reaction–diffusion systems. J. Dyn. Differ. Equ. **12**, 117–167 (2000)
- Ikeda, T., Ikeda, H., Mimura, M.: Hopf bifurcation of travelling pulses in some bistable reaction–diffusion systems. Methods Appl. Anal. **7**, 165–193 (2000)
- Ikeda, H., Mimura, M., Nishiura, Y.: Global bifurcation phenomena of traveling wave solutions for some bistable reaction–diffusion systems. Nonlinear Anal. **13**, 507–526 (1989)
- Khlebnik, A.I., Krauskopf, B., Rousseau, C.: Global study of a family of cubic Lienard equations. Nonlinearity **11**, 1505–1519 (1998)
- Knobloch, E.: Normal forms for bifurcations at a double zero eigenvalue. Phys. Lett. A **115**, 199–201 (1986)
- Kolokolnikov, T., Ward, M.J., Wei, J.: Zigzag and breakup instabilities of stripes and rings in the two-dimensional Gray–Scott Model. Stud. Appl. Math. **16**, 35–95 (2006)
- Krupa, M.: Bifurcations of relative equilibria. SIAM J. Math. Anal. **21**, 1453–1486 (1990)
- Meron, E., Bär, M., Hagberg, A., Thiele, U.: Front dynamics in catalytic surface reactions. Catalysis Today **70**, 331–340 (2001)
- Meron, E.: Nonlinear Physics of Ecosystems. CRC Press, Boca Raton (2015)
- Nishiura, Y., Fujii, H.: Stability of singularly perturbed solutions to systems of reaction–diffusion equations. SIAM J. Math. Anal. **18**, 1726–1770 (1987)
- Nishiura, Y., Mimura, M.: Layer oscillations in reaction–diffusion systems. SIAM J. Appl. Math. **49**, 481–514 (1989)
- Nishiura, Y., Mimura, M., Ikeda, H., Fujii, H.: Singular limit analysis of stability of traveling wave solutions in bistable reaction–diffusion systems. SIAM J. Math. Anal. **21**, 85–122 (1990)
- Nishiura, Y., Teramoto, T., Ueda, K.-I.: Scattering and separators in dissipative systems. Phys. Rev. E **67**, 056210 (2003)
- Nishiura, Y., Teramoto, T., Yuan, X., Ueda, K.-I.: Dynamics of traveling pulses in heterogeneous media. Chaos **17**, 037104 (2007)
- Nishiura, Y., Ueyama, D.: Spatio-temporal chaos for the Gray–Scott model. Physica D **150**, 137–162 (2001)
- Or-Guil, M., Bode, M., Schenk, C.P., Purwins, H.-G.: Spot bifurcations in three-component reaction–diffusion systems: the onset of propagation. Phys. Rev. E **57**, 6432–6437 (1998)
- Pearson, J.E.: Complex patterns in a simple system. Science **261**, 189–192 (1993)
- Purwins, H.-G., Stollenwerk, L.: Synergetic aspects of gas-discharge: lateral patterns in DC systems with a high ohmic barrier. Plasma Phys. Controll. Fus. **56**, 123001 (2014)
- Promislow, K.: A renormalization method for modulational stability of quasi-steady patterns in dispersive systems. SIAM J. Math. Anal. **33**, 1455–1482 (2002)
- Rademacher, J.D.M.: First and second order semi-strong interaction in reaction-diffusion systems. SIAM J. Appl. Dyn. Syst. **12**, 175–203 (2013)

- Rademacher, J.D.M., Uecker, H.: Symmetries, freezing, and Hopf bifurcations of traveling waves in pde2path (2017). <http://www.staff.uni-oldenburg.de/hannes.uecker/pde2path/tuts/symtut.pdf>. Accessed 10 July 2019
- Sandstede, B.: Stability of traveling Waves. Handbook of Dynamical Systems, vol. 2. North-Holland, Amsterdam (2002)
- Sandstede, B., Scheel, A., Wulff, C.: Dynamics of spiral waves on unbounded domains using center-manifold reductions. *J. Differ. Equ.* **141**, 122–149 (1997)
- Schenk, C.P., Or-Guil, M., Bode, M., Purwins, H.-G.: Interacting pulses in three-component reaction–diffusion systems on two-dimensional domains. *Phys. Rev. Lett.* **78**, 3781–3784 (1997)
- Sun, W., Ward, M.J., Russell, R.: The slow dynamics of two-spike solutions for the Gray–Scott and Gierer–Meinhardt systems: competition and oscillatory instabilities. *SIAM J. Appl. Dyn. Syst.* **4**, 904–953 (2005)
- Uecker, H., Wetzel, D., Rademacher, J.D.M.: pde2path—a Matlab package for continuation and bifurcation in 2D elliptic systems. *NMTMA* **7**, 58–106 (2014)
- van Heijster, P., Chen, C.-N., Nishiura, Y., Teramoto, T.: Localized patterns in a three-component FitzHugh–Nagumo model revisited via an action functional. *J. Dyn. Differ. Equ.* **30**, 521–555 (2018)
- van Heijster, P., Chen, C.-N., Nishiura, Y., Teramoto, T.: Pinned solutions in a heterogeneous three-component FitzHugh–Nagumo model. *J. Dyn. Differ. Equ.* **31**, 153–203 (2019)
- van Heijster, P., Doelman, A., Kaper, T.J.: Pulse dynamics in a three-component system: stability and bifurcations. *Physica D* **237**, 3335–3368 (2008)
- van Heijster, P., Doelman, A., Kaper, T.J., Promislow, K.: Front interactions in a three-component system. *SIAM J. Appl. Dyn. Syst.* **9**, 292–332 (2010)
- van Heijster, P., Doelman, A., Kaper, T.J., Nishiura, Y., Ueda, K.-I.: Pinned fronts in heterogeneous media of jump type. *Nonlinearity* **24**, 127–157 (2011)
- van Heijster, P., Sandstede, B.: Planar radial spots in a three-component FitzHugh–Nagumo system. *J. Nonlinear Sci.* **21**, 705–745 (2011)
- van Heijster, P., Sandstede, B.: Bifurcations to traveling planar spots in a three-component FitzHugh–Nagumo system. *Physica D* **275**, 19–34 (2014)
- Vanag, V.K., Epstein, I.R.: Localized patterns in reaction–diffusion systems. *Chaos* **17**, 037110 (2007)
- Veerman, F.: Breathing pulses in singularly perturbed reaction–diffusion systems. *Nonlinearity* **28**, 2211–2246 (2015)